Bulky Diphosphite-Modified Rhodium Catalysts: Hydroformylation and Characterization

Annemiek van Rooy,[†] Paul C. J. Kamer,[†] Piet W. N. M. van Leeuwen,*[,†] Kees Goubitz,[‡,§] Jan Fraanje,[‡] Nora Veldman,[||] and Anthony L. Spek[||,⊥]

Van 't Hoff Research Institute, Department of Inorganic Chemistry, University of Amsterdam, Nieuwe Achtergracht 166, 1018 WV Amsterdam, The Netherlands, Amsterdam Institute for Molecular Studies, Department of Crystallography, University of Amsterdam, Nieuwe Achtergracht 166, 1018 WV Amsterdam, The Netherlands, and Bijvoet Center for Biomolecular Research, Vakgroep Kristal- en Structuurchemie, Utrecht University, Padualaan 8, 3584 CH Utrecht, The Netherlands

Received July 18, 1995[⊗]

The rhodium-catalyzed hydroformylation with the diphosphites P[O(2,2′-(4-X-6-Y-C_6H_2)$_2$O]-[O(2,2′-(4-X-6-Y-C_6H_2)$_2$)OP][O(4-Z-C_6H_4)$_2$ (X = Y = *tert*-butyl, Z = H (**1**), Z = OMe (**2**), Z = C_6H_5 (**3**), Z = Cl (**4**); X = OMe, Y = *tert*-butyl, Z = H (**5**)), [PO(2,2′-(4,6-(*tert*-C_4H_9)$_2$$C_6H_2$)$_2$)O]$_2$R [R = O($CH_2$)$_2$O (**6**), R = O($CH_2$)$_3$O (**7**)], [PO(2,2′-($C_6H_4$)$_2$)O]$_2$R, R = O(2,2′-(4-MeO-6-*tert*-$C_4H_9C_6H_2$)$_2$O (**8**), R = O(2,2′(4,6-*tert*-C_4H_9)$_2$$C_6H_2$)$_2$O (**9**)], and [PO(2,2′-(4,6-(*tert*-C_4H_9)$_2$-C_6H_2)$_2$)O]$_2$[O(2,2′-(C_6H_4)$_2$)O] (**10**) as ligands is studied with oct-1-ene and styrene as substrates. For oct-1-ene the highest normal to branched ratio obtained is 48 (**5**). For styrene the product selectivity depends strongly on the reaction temperature; a branched to normal ratio of 19 is found for **7** when T = 40 °C *vs* a branched to normal ratio of 0.19 for **1** when T = 120 °C. A bulky and bisequatorially (ee) coordinating diphosphite is required to obtain a high regioselectivity for linear aldehydes, while flexible diphosphites or equatorially−axially (ea) coordinating diphosphites lead to an enhancement of the formation of branched aldehydes. The hydroformylation of oct-1-ene has a first-order dependency in the oct-1-ene concentration, the order in CO is approximately −0.65, and the order in H_2 is approximately 0.2. This is consistent with a kinetic scheme in which alkene addition is the rate-determining step. The crystal structures of RhAcac(**4**) and RhH(CO)$_2$(**4**) (**11**), are presented. The hydrido ligand in **11** could not be located. The structure reveals a distorted TBP with **4** ee coordinated, the P(1)−Rh−P(2) angle being 115.95(9)°. The distortion is indicative of a crowded rhodium center which explains the obtained high linearity of the hydroformylation products.

Introduction

Since Wilkinson's discovery that through addition of phosphorus ligands rhodium-catalyzed hydroformylation can be performed at lower temperatures and pressures,[1] much research has been done to develop ligands that increase the rate and the regioselectivity of the reaction. During the last several years it has become apparent that these improvements can be effected with bidentate ligands, and research has concentrated on chelating ligands such as diphosphines, ether−phosphane ligands, and diphosphinite ligands.[2] Chiral diphosphines proved to be applicable in the rhodium-catalyzed enantioselective hydroformylation of prochiral substrates.[3] A general problem of these ligands is their sensitivity toward oxidation. Phosphite ligands, however, are relatively inert toward oxidation and easy to synthesize. Recently we found that the rhodium catalyst precursor modified by a bulky monophosphite increased the reactivity enormously, but a moderate regioselectivity was obtained.[4] From patents and recent literature[5] it is known that bulky diphosphites give rise to very selective hydroformylation catalysts. We suggested earlier that the regioselectivity in the hydroformylation of unsubstituted 1-alkenes is

† Van't Hoff Research Institute.
‡ Amsterdam Institute for Molecular Studies.
§ Address correspondence pertaining to the crystallographic study of RhAcac(**4**) to this author.
|| Bijvoet Center for Biomolecular Research.
⊥ Address correspondence pertaining to the crystallographic study of **11** to this author.

⊗ Abstract published in *Advance ACS Abstracts,* December 15, 1995.

(1) (a) Slaugh, L. H.; Mullineaux, R. D. U.S. Pat. 3 239 566, 1966. (b) Eiseman, J. L. U.S. Pat. 3 290 379 1966. (c) Evans, D.; Osborn, J. A.; Wilkinson, G. J. *J. Chem. Soc. A* **1968**, 3133. Yagupski, G.; Brown, C. K.; Wilkinson, G. J. *J. Chem. Soc. A* **1970**, 1392. Brown, C. K.; Wilkinson, G. J. *J. Chem. Soc. A* **1970**, *2753*.

(2) (a) Casey, C. P.; Whitteker, G. T.; Melville, M. G.; Petrovich, L. M.; Gavney, J. A., Jr.; Powell, D. R. *J. Am. Chem. Soc.* **1992**, *114*, 5535. (b) Consiglio, G.; Rama, F. *J. Mol. Catal.* **1991**, *66*, 1. (c) Del Zotto, A.; Costella, L.; Mezzetti, A.; Rigo, P. *J. Organomet. Chem.* **1991**, *414*, 109. (d) Trzeciak, A.; Ziolkowski, J. J. *J. Organomet. Chem.* **1991**, *420*, 353. (e) Alper, H.; Zhou, J.-Q. *J. Chem. Soc., Chem. Commun.* **1993**, 317. (f) Lindner, E.; Norz, H. *Chem. Ber.* **1990**, *123*, 459. (g) Lindner, E.; Glaser, E. *J. Organomet. Chem.* **1990**, *391*, C37. (h) Selke, R. *J. Organomet. Chem.* **1989**, *370*, 241. (i) Valderama, M.; Scott, M.; Abugoch, L. *J. Coord. Chem.* **1990**, *21*, 55. (j) Pottier, Y.; Mortreux, A.; Petit, F. *J. Organomet. Chem.* **1989**, *370*, 333. (k) Baker, M. J.; Pringle, P. G. *J. Chem. Soc., Chem. Commun.* **1993**, 314. (l) Devon, T. J.; Phillips, G. W.; Puckette, T. A.; Stavinoha, J. L.; Vanderbilt, J. J. U.S. Pat. 4 694 109, 1989 (to Eastman Kodak). (m) Unruh, J. D.; Christenson, J. R. *J. Mol. Catal.* **1982**, *14*, 19.

(3) (a) Salomon, C.; Consiglio, G.; Botteghi, C.; Pino, P. *Chimia* **1973**, *27*, 215. (b) Stern, R.; Hirschauer, A.; Sajus, L. *Tetrahedron Lett.* **1973**, *35*, 3247. (c) Tanaka, M.; Ikeda, Y.; Ogata, I. *Chem. Lett.* **1975**, 1115. Hayashi, T.; Tanaka, M.; Ikeda, Y.; Ogata, I. *Bull. Chem. Soc. Jpn.* **1979**, *52*, 2605. (d) Becker, Y.; Eisenstadt, A.; Stille, J. K. *J. Org. Chem.* **1980**, *45*, 2145. (e) Gladiali, S.; Pinna, L. *Tetrahedron: Asymmetry* **1990**, *1*, 693.

(4) (a) Van Rooy, A.; Orij, E. N.; Kamer, P. C. J.; Van den Aardweg, F.; Van Leeuwen, P. W. N. M. *J. Chem. Soc., Chem. Commun.* **1991**, 1096. (b) Van Rooy, A.; Orij, E. N.; Kamer, P. C. J.; Van Leeuwen, P. W. N. M. *Organometallics* **1995**, *14*, 34.

0276-7333/96/2315-0835$12.00/0

caused by an equatorial−equatorial (ee) coordination of both the phosphorus atoms.[6] This coordination would be induced by a natural bite angle of the diphosphite of approximately 120°, as was hypothesized by Casey *et al.* for diphosphine ligands.[2a] Recently, the first studies of asymmetric rhodium-catalyzed hydroformylation with chiral diphosphite ligands were published.[7] Although no data on the mechanistic and kinetic behavior of catalysts modified by bidentate ligands are as yet available, it is commonly accepted that the mechanism for the cobalt-catalyzed hydroformylation as postulated by Heck and Breslow[8] can be applied to ligand-modified rhodium carbonyl as well. It is also assumed that the addition of the alkene to the hydrido−rhodium complex or one of the early migration steps is the rate-limiting step. Kinetic studies indicate the same for the triphenylphosphine-modified system.[9] These studies are in contrast with the persisting assumption[10] that the H_2 addition is the rate-determining step. This was found by Wilkinson who studied the rhodium triphenylphosphine catalyst at low pressures (<1 bar).[1c] Under higher pressures that are more comparable to real process conditions the alkene addition becomes rate limiting. Recently Gladfelter concluded that the regioselectivity of the product aldehyde was not determined during the alkene insertion, but these results were obtained under mass transfer limiting conditions.[11]

We started a fundamental study of the influence of the structure of various diphosphites on the rhodium-catalyzed hydroformylation reaction. We tested some of the diphosphites that were recently reported by the Union Carbide Co. (**1**−**10**)[5a] (Chart 1) as modifying ligands in the hydroformylation of oct-1-ene and styrene and compared the rates and product selectivities. With **4** a kinetic study was performed involving the influence of several reaction parameters on the rate and selectivity of the hydroformylation of oct-1-ene. We elucidated the structure of several of the catalysts under process conditions in order to find a relationship between the structure and the catalytic and kinetic performance. To gain information on possible intermediates and to propose a mechanism for the formation of the active catalyst complex, we studied the reaction of the precursor and the ligands with and without addition of syngas pressure and characterized the formed complexes spectroscopically.

Chart 1

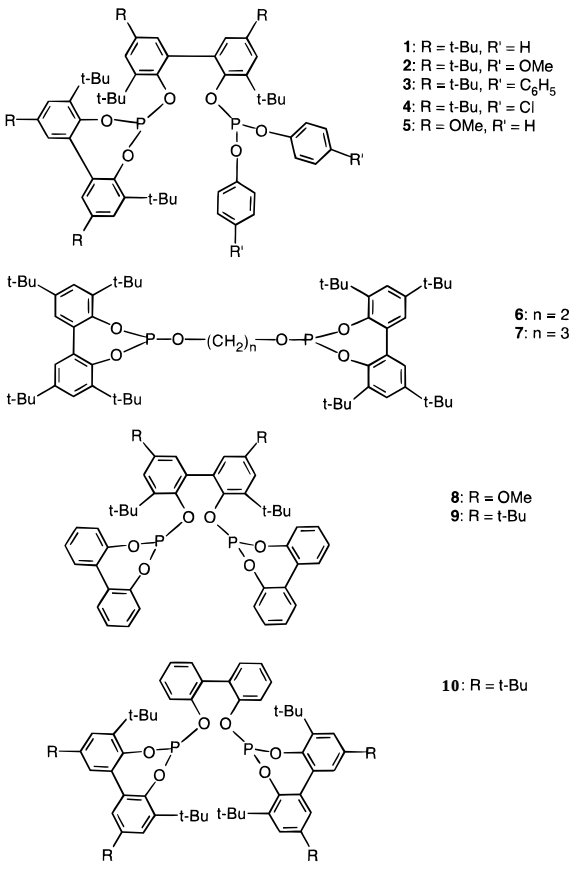

Results and Discussion

Hydroformylation of Oct-1-ene and Styrene. Oct-1-ene. The hydroformylation of oct-1-ene with rhodium catalysts containing the bulky diphosphites **1**−**5** occurs with a regular reaction rate (average rate ≈ 2500 mol (mol of Rh)$^{-1}$ h^{-1}, T = 80 °C, 0.4 mM Rh, PP/Rh = 20, 20 mmol of oct-1-ene in 20 mL of toluene; see Table 1) and a very high selectivity for the linear aldehyde (up to a normal/branched ratio of 48 for **5**). The amount of isomerized oct-1-ene varied from 0% (**2**−**4**) to 23% (**1**). Variation of the para substituent on the phenyl ring on the less bulky phosphorus atom (P_2), in order to modify the electron-donating ability, appears to be of little or no influence on the rate and the regioselectivity. Diphosphites **8** and **9**, with only bulky groups on the bridge between the two phosphorus atoms, give rise to even more selective catalysts (no branched aldehydes were detected for **8**) although the isomerization rate is high (18 and 26.5%, respectively). Recently high isomerization rates were also reported by Gladfelter[11] under mass transfer limiting conditions. The lack of isomerization found with **2**−**4** is probably a consequence of a faster CO addition and subsequent migration compared to β-H elimination under our reaction conditions. Buchwald found no isomerization in the rhodium-catalyzed hydroformylation of a variety of

(5) (a) Billig, E.; Abatjoglou, A. G.; Bryant, D. R. U.S. Pat. 4 769 498, 1988 (to Union Carbide). (b) Baker, M. J.; Harrison, K. N.; Orpen, A. G.; Pringle, P. G.; Shaw, G. *J. Chem. Soc., Chem. Commun.* **1991**, 803. (c) Lorz, P. M. Eur. Pat. 0 472 071 A1, 1991. (d) Cuny, G. D.; Buchwald, S. L. *J. Am. Chem. Soc.* **1992**, *115*, 2066−2068. (e) Moasser, B.; Gladfelter, W. L. Presented at the 206th ACS National Meeting, Chicago, IL, 1993; poster 371.

(6) Van Leeuwen, P. W. N. M.; Buisman, G. J. H.; Van Rooy, A.; Kamer, P. C. *J. Recl. Trav. Chim. Pays Bas* **1994**, 1.

(7) (a) Buisman, G. J. H.; Kamer, P. C. J.; Van Leeuwen, P. W. N. M. *Tetrahedron: Asymmetry* **1993**, *4*, 1625. (b) Babin, J. E.; Whiteker, G. T. W. O. 93 03839, U.S. Pat. 911 518, 1992 (to Union Carbide Corp.). (c) Buisman, G. J. H.; Vos, E.; Kamer, P. C. J.; Van Leeuwen, P. W. N. M. *J. Chem. Soc., Dalton Trans.* **1995**, 409. (d) Buisman, G. J. H. Ph.D. Thesis, University of Amsterdam, 1995.

(8) Heck, R. F.; Breslow, D. S. *J. Am. Chem. Soc.* **1961**, *83*, 4023.

(9) (a) Cavalieri d'Oro, P.; Raimondt, L.; Pagani, G.; Montrasi, G.; Gregorio, G.; Oliveri del Castillo, G. F.; Andreeta, A. *Symp. Rhodium Homogeneous Catal., Proc.* **1978**; 76−83. (b) Gregorio, G.; Montrasi, G.; Tampieri, M.; Cavalieri d'Oro, P.; Pagani, G.; Andreetta, A. *Chim. Ind.* **1980**, *62* (5), 389. Cavalieri d'Oro, P.; Raimondi, L.; Pagani, G.; Montrasi, G.; Gregorio, G.; Andreetta, A. *Chim. Ind.* **1980**, *62* (7−8), 572. (c) Van Leeuwen, P. W. N. M.; Van Koten, G. *Catalysis. An Integrated Approach to Homogeneous, Heterogeneous and Industrial Catalysis*, 2nd ed.; Moulijn, J. A.; Van Leeuwen, P. W. N. M., Van Santen, R. A., Eds.; Elsevier: Amsterdam, London, New York, Tokyo, 1995; pp 199−222.

(10) (a) Collman, J. P.; Hegedus, L. S.; Norton, J. R.; Finke, R. G. *Principles and Applications of Organotransition Metal Chemistry*, 2nd ed.; University Science Books: Mill Valley, CA, 1987. (b) Tolman, C. A.; Faller, J. W. *Homogeneous Catalysis with Metal Phosphine Complexes*; Pignolet, L. H., Ed.; Plenum Press: New York and London, 1983; Chapter 2, pp 88−89.

(11) Moasser, B.; Gladfelter, W. L. *Organometallics* **1995**, *14*, 3832.

Table 1. Results of the Hydroformylation of Oct-1-ene with $Rh(CO)_2Acac$ and Various Diphosphites as Catalyst Precursors[a]

diphosphite	conversion (%)	product distribution (%)			TOF[f] (mol (mol of RH)$^{-1}$ h^{-1})
		isomerized oct-1-ene	normal	branched	
1	26	23	73	4	2450
2	29	*b*	96	4	2700
3	19	*b*	95	5	2275
4	21	*b*	95	5	3375
5	35	16	82.3	1.7	1750
6	21	*b*	61.5	38.5	11100
7[c]	27	20	55	25	1550
7[d]	27	7	50	43	130
8[e]	31	18	82	*b*	3600
9	37	26.5	72.1	1.4	6120
10	21	13	48	39	520

[a] Conditions: $T = 80$ °C, 0.4 mM of $Rh(CO)_2Acac$, diphosphite/Rh = 20, $P_{H_2} = P_{CO} = 10$ bar, 20 mmol of 1-octene in 20 mL of toluene. [b] Not detected. [c] Diphosphite/Rh = 2.5. [d] $T = 40$ °C. [e] Diphosphite/Rh = 16. [f] Averaged over the conversion.

alkenes with **8** as ligand, but these experiments were performed at room temperature.[5d] Addition of the diphosphites with flexible alkyl bridges, **6** and **7**, results for **6** in an increase of the reaction rate with a factor of 3 (11 100 mol (mol of Rh)$^{-1}$ h^{-1}), but the regioselectivity decreases enormously (normal/branched (n/b) = 1.6). Diphosphite **10**, less bulky than **1**−**5**, and in contrast with **6** and **7** containing a rigid bridging group, gives both a low product linearity and a low reaction rate.

The rigid diphosphites show rates lower than most of the monodentate phosphorus ligand systems (*e.g.* PPh_3, 5000 mol [mol of Rh]$^{-1}$ h^{-1}, 5% v/v in benzene, 0.5 mM Rh, PPh_3/Rh = 10, 90 °C, 20 bar syngas; tris(2-*tert*-butyl-4-methylphenyl) phosphite, 40 000 mol (mol of Rh)$^{-1}$ h^{-1}, 20 mmol of oct-1-ene in 20 mL of toluene, 0.1 mM Rh, P/Rh = 50 (P = tris(2-*tert*-butyl-4-methylphenyl) phosphite), $T = 80$ °C),[4b] but they react faster than other bidentate ligands (DPPE (DPPE = 1,2-bis(diphenylphosphino)ethane), 100 mol (mol of Rh)$^{-1}$ h^{-1}, $n/b = 1$, 0.4 mM Rh,[12] DPPE/Rh = 10, $T = 80$ °C, 20 bar CO/H_2; BISBI (BISBI = 2,2′-bis(diphenylphosphinomethyl)(1,1′-biphenyl)), 850 mol (mol of Rh)$^{-1}$ h^{-1}, $n/b = 80$, 1.78 mM Rh, BISBI/Rh = 2.2, 10 bar, $T = 80$ °C, 0.01 mol of oct-1-ene[13]). The rigid diphosphites react with equal (BISBI) or higher (DPPE) selectivity to the linear product. The catalysts with the flexible diphosphites react with rates and selectivities equal to those of the triphenylphosphine-modified system.[14] Hydrogenation of alkenes above the detection limit (0.1%) was not observed in any of the studied catalyst systems.

Comparison of diphosphites **6** and **7** with **1**−**5** and **8** and **9** suggests that the rigid and sterically demanding bridge between the phosphorus atoms is responsible for the high regioselectivity rather than the large substituents at the phosphorus atoms.

Styrene. In the hydroformylation of styrene with ligands **1**−**4** (Table 2), the reaction rates are generally a factor of 10 lower than those for oct-1-ene (average rates of ≈300 mol (mol of Rh)$^{-1}$ h^{-1}, $T = 80$ °C, 20 mmol of styrene in 20 mL of toluene; around 50 mol (mol of Rh)$^{-1}$ h^{-1} for $T = 40$ °C), and we obtained very low selectivities for the formation of the branched 2-phenylpropanal with the rigid diphosphites **1**−**4** and **8**, the branched to normal ratio being almost 1. Lowering the reaction temperature did increase the formation of the branched aldehyde, but the regioselectivity remained moderate. Apparently, use of these diphosphites leads, as also found for oct-1-ene, toward an increase of the selectivity to the linear aldehydes. Thus, when higher temperatures were used, a large excess of the linear aldehydes was now observed; at a reaction temperature of 120 °C, a selectivity of 84% for the linear phenylpropanal was found (hydrogenation not taken into account, the highest selectivity for the formation of 2-phenylpropanal reported so far is 70%[13,15]).

Table 2. Results of the Hydroformylation of Styrene with $Rh(CO)_2Acac$ and Various Diphosphites as Catalyst Precursors[a]

diphosphite	conversion (%)	normal aldehyde (%)	brnached aldehyde (%)	TOF[b] (mol (mol of Rh)$^{-1}$ h^{-1})
1	22	49	51	330
1[c]	13	16	84	47
1[d]	13	84	16	6175 (16% ethylbenzene)
d	3	73	27	1075 (27% ethylbenzene)
d	32	68	32	350 (32% ethylbenzene)
2	25	37	63	320
3	18	49	51	320
6	25	12	88	3710
7[c,e]	31	5	95	30
7[e]	31	16	84	1890
8[c]	27	23	77	47

[a] Conditions: $T = 80$ °C, 0.4 mM of $Rh(CO)_2Acac$, diphosphite/Rh = 20, $P_{H_2} = P_{CO} = 10$ bar, 20 mmol of styrene in 20 mL of toluene. [b] Turnover frequencies for the formation of aldehydes averaged over conversion. [c] $T = 40$ °C. [d] $P_{CO} = 5$ bar, $P_{H_2} = 30$ bar, $T = 120$ °C. [e] Diphosphite/Rh = 2.5.

Due to its specific electronic properties styrene is known to show a natural preference for forming the branched (1-phenylethyl)rhodium compound and hence a high selectivity for the branched aldehyde. For bidentate ligands high b/n ratio's were often reported.[7,16] However, application of the rigid diphosphites gives rise to a catalyst with a different selectivity. The pressure- and temperature-dependent product distribution suggests that the branched rhodium complex, when formed, undergoes β-H elimination and re-forms the starting alkene and hydridorhodium complex. From Lazzaroni's work[15] it is known that branched alkylrhodium intermediates are more sensitive toward β-H elimination than the linear alkyl complexes; especially for styrene this difference in sensitivity is large. This is often suggested to be caused by the stabilization of an (η^3-styryl)rhodium intermediate;[10b] although these intermediates were already demonstrated for several metals,[17] it has not been until recently that the first (η^3-styryl)rhodium complex was isolated.[18] Wink[16] argued that in his rhodium diphosphite systems η^3-styryl species do not play a role, although he obtained high b/n ratios (97% branched aldehyde), which is in concert with the small size of the unsubstituted bisnaphthol diphosphites.

(12) De Lange, W. G. J.; Kamer, P. C. J.; Van Leeuwen, P. W. N. M. Unpublished results (8 μmol of $Rh(CO)_2Acac$, 80 μmol of DPPE, 20 mmol of oct-1-ene, 20 bar of CO/H_2, 80 °C, in 20 mL of toluene: TOF = 100 mol (mol of Rh)$^{-1}$ h^{-1}; $n/b = 1$).

(13) Kranenburg, M.; Van der Burgt, Y. E. M.; Kamer, P. C. J.; Van Leeuwen, P. W. N. M. *Organometallics* **1995**, *14*, 3081.

(14) Van Rooy, A.; De Bruijn, J. N. H.; Roobeek, K. F.; Kamer, P. C. J.; Van Leeuwen, P. W. N. M. *J. Organomet. Chem.* **1995**, in press.

(15) A 65% value was reported by: Lazzaroni, R.; Raffaelli, A.; Settambolo, R.; Bertozzi, S.; Vituli, G. *J. Mol. Catal.* **1989**, *50*, 1.

(16) Kwok, T. J.; Wink, D. J. *Organometallics* **1993**, *12*, 1954.

(17) Crascall, L. E.; Litster, S. A.; Redhouse, A. D.; Spencer, J. L. *J. Organomet. Chem.* **1990**, *394*, C35.

(18) Schäfer, M.; Mahr, N.; Wolf, J.; Werner, H. *Angew. Chem.* **1993**, *32*, 1315.

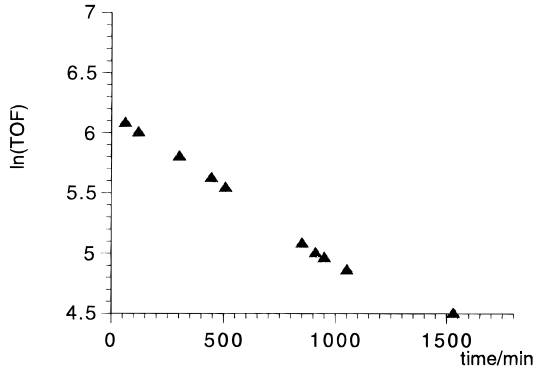

Figure 1. Plot of ln(TOF) *vs* the reaction time. Conditions: $T = 60$ °C, $P_{H_2} = P_{CO} = 10$ bar, 0.4 mM $Rh(CO)_2$-Acac, **4**/Rh = 10, 20 mmol of oct-1-ene in 20 mL of toluene.

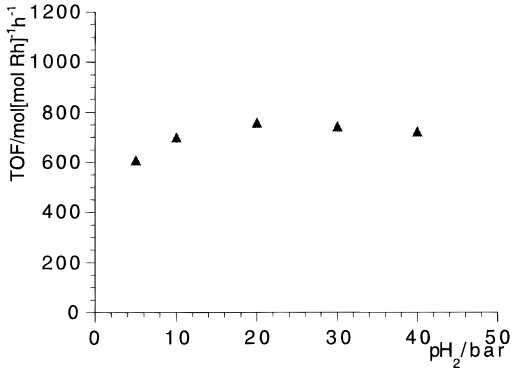

Figure 2. Dependency of the reaction rate on the H_2 pressure of the hydroformylation of oct-1-ene. Conditions: $T = 60$ °C, $p_{CO} = 10$ bar, 0.4 mM $Rh(CO)_2$Acac, **4**/Rh = 10, 20 mmol of oct-1-ene in 20 mL of toluene.

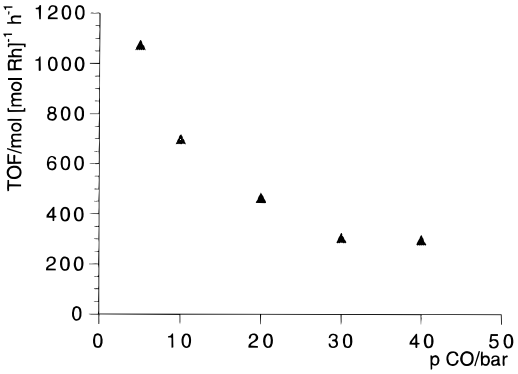

Figure 3. Dependency of the reaction rate on the CO pressure of the hydroformylation of oct-1-ene. Conditions: $T = 60$ °C, $P_{H_2} = 10$ bar, 0.4 mM $Rh(CO)_2$Acac, **4**/Rh = 10, 20 mmol of oct-1-ene in 20 mL of toluene.

As low CO pressures and high temperatures facilitate β-H elimination, β-H elimination eventually dominates hydroformylation of the branched alkylrhodium complex. Since formation of the linear (2-phenylethyl)-rhodium remains irreversible at low pressures and high temperatures, the product selectivity shifts toward the normal aldehyde as we indeed observed (see Table 2).

The use of diphosphites **6** and **7** with an aliphatic, flexible bridging chain as auxiliary ligands resulted in higher rates (3710 mol (mol of Rh)$^{-1}$ h^{-1} for **6**) and higher regioselectivities for the branched aldehydes: a branched to normal ratio up to 19 for the five-membered bridge (**7**). This is in agreement with the preference for the formation of the branched (1-phenylethyl)rhodium intermediate when there are no steric constraints.

Cyclohexene. When we tried to hydroformylate cyclohexene with the bulky diphosphite-modified catalyst, higher pressures were required to reach any conversion at all, but even under these conditions reaction rates remained very low (TOF = 150 mol (mol of Rh)$^{-1}$ h^{-1}, **1**, $T = 80$ °C, $P_{CO} = P_{H_2} = 40$ bar). A bulky and monodentate ligand is required to obtain acceptable rates; *e.g.*, with tris(2-*tert*-butyl-4-methylphenyl) phosphite as a ligand a rate of 512 mol (mol of Rh)$^{-1}$ h^{-1} was obtained ($T = 80$ °C, $P_{CO} = P_{H_2} = 10$ bar, initial cyclohexene concentration = 0.91 M).[4b]

Kinetic Study. We decided to study the influence of the reaction parameters with one of the diphosphite ligands that gave a high selectivity for the linear aldehyde in the hydroformylation of oct-1-ene. We collected kinetic data for the reaction of the ligand **4** modified catalyst, and the results are given in Figures 1−3. As can be concluded from the plot of the ln(TOF) *vs* reaction time (Figure 1), the reaction is first order with respect to the oct-1-ene concentration. The rate constant shows almost no dependency on the H_2 pressure (≈0.2) (Figure 2) and a clear negative order in the CO concentration. The order in CO showed to be −0.65 (Figure 3). This suggests that the first step in the reaction cycle, the exchange of a CO ligand for a π-coordinated alkene, is rate-limiting.[19]

These results are almost equal to the kinetic expression of the PPh_3-modified catalyst. In this active hydridorhodium complex, at least two phosphine ligands are coordinated to the rhodium metal. Cavalieri d'Oro,[9a,b] one of the few who studied the kinetics of the triphenylphosphine-modified hydroformylation of propene under real process conditions (*i.e.* 2−70 bar, 90−110 °C), found that the reaction rate increased with increasing alkene concentration and observed a very low order in the dependencies on both the CO and H_2 concentration. This different order in CO concentration can be explained by the nature of the phosphorus ligands; in the triphenylphosphine system either a molecule of CO or a phosphine ligand can dissociate (depending on the amount of phosphine ligands coordinated) to allow the addition of the substrate. At higher CO pressures the reaction rate hardly decreases implying that a phosphine ligand is replaced by the alkene molecule. This is also supported by a negative order in the PPh_3 concentration.[20] As follows from the large negative order in the CO concentration in the diphosphite-modified system, a CO molecule dissociates after which the alkene can coordinate. In mononuclear systems with $HRh(CO)_4$ and $HRh(CO)_3P$ as the active catalysts, the rate expression for 1-alkenes is different from that for catalysts with diphosphites or PPh_3.[4b,21] Here, a zeroth-order dependency in the substrate concentration and a first-order dependency with respect to the H_2 pressure were observed. This means that the rate-limiting step is now the reaction of the rhodium acyl complex with H_2.

Another remarkable result of the diphosphite-modified catalyst is the decrease in selectivity for the linear

(19) We have not attempted to find an analytic expression for the rate in view of the large number of steps involved. See ref 4b for analytical derivations for part of the reaction scheme.

(20) Jardine, F. *Polyhedron* **1982**, 569.

(21) Marko, L. *Aspects of homogeneous catalysis*; Ugo, R., Ed.; Reidel: Dordrecht and Boston, 1973; Vol. 2, Chapter 1.

Scheme 1. Hydroformylation *vs* Isomerization

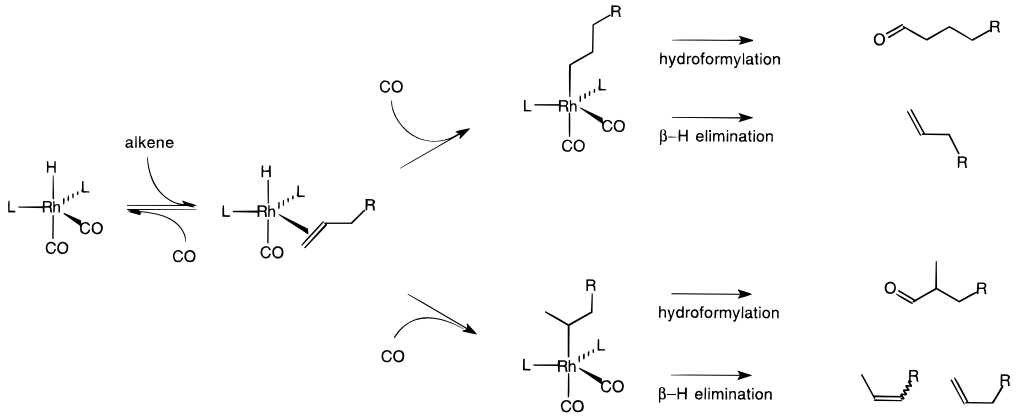

Table 3. Influence of the CO Pressure on the *n*/*b* Ratio and the Amount of Isomerization[a]

P_{CO}	normal aldehyde (%)	branched aldehyde (%)	isomerization (%)
5	87	3	10
10	87	6	7
20	84	10	6
30	78	15	7
40	75	19	6

[a] Conditions: $T = 60$ °C, 0.4 mM $Rh(CO)_2Acac$, **4**/Rh = 10, P_{H_2} = 10 bar, 20 mmol of 1-octene in 20 mL of toluene.

nonanal at increasing CO pressure (see Table 3). The normal to branched ratio drops from 29 at $P_{CO} = 5$ bar to 4 at $P_{CO} = 40$ bar, while the isomerization decreases from 10% to 6%.

Isomerization of the alkene only occurs when β-H elimination of the *branched* alkylrhodium compound takes place (see Scheme 1); β-H elimination of the *linear* alkylrhodium species re-forms the 1-alkene. This β-H elimination reaction, facilitated at low CO pressures, converts the branched alkylrhodium into 2-alkenes. Thus, at low pressures, a substantial amount of the branched alkylrhodium complex does not proceed to form the branched aldehydes and consequently (at incomplete conversions) the *n*/*b* ratio increases. However, the decreasing isomerization rate at high CO pressures cannot totally account for the loss of selectivity. The presence of rhodium complexes that contain only one or even no rhodium−phosphorus bonds can explain these results as such species are expected to react with low selectivity and high rate. In addition, the relatively high rate of these complexes compared to complexes with bidentate diphosphites can disturb the reaction kinetics.

Catalyst Characterization Experiments. Reactions of $Rh(CO)_2Acac$. In order to identify the catalyst complex and the possible intermediates during its formation, we added 1 equiv of **4** to the $Rh(CO)_2Acac$ precursor. Immediately, one CO ligand is substituted with the least sterically hindered phosphorus atom (**A**)

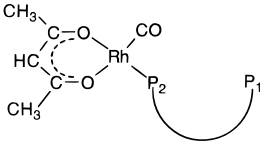

A

as is concluded from the upfield shift of its $\delta(^{31}P)$ value

Table 4. ^{31}P NMR Data for Rh(Acac)(CO)(diphosphite) and Rh(Acac)(diphosphite) (Benzene-d_6)

	$\delta(^{31}P_1)$ (ppm)	J_{RhP1} (Hz)	$\delta(^{31}P_2)$ (ppm)	J_{RhP2} (Hz)	J_{P1P2} (Hz)
			Rh(Acac)(CO)(diphosphite)		
1	126.2	295	141.0		6
2[a]	126.8	296	141.2		6
4	127.5	296	141.1		6
			Rh(Acac)(diphosphite)		
1[a]	134.8	301	130.3	309	110
2[a]	135.7	298	131.6	311	107
4[b]	134.0	296	130.8	284	109
6	144.8	307			
8	146.7	296			

[a] Toluene-d_8. [b] $CDCl_3$.

(≈20 ppm) and its rhodium−phosphorus coupling constant of ≈296 Hz. The chemical shift of the noncoordinating phosphorus has changed very slightly compared to the free ligand, and the coupling constant between P_1 and P_2 equals that of the free diphosphite (6 Hz). In the IR spectrum, the two CO stretch vibrations of $Rh(CO)_2Acac$ (2080, 2012 cm^{-1}) are replaced by one vibration at 2015 cm^{-1}. Data for several of these complexes are given in Table 4.

For the nonsymmetric bulky diphosphites only after heating or evacuating the mixture, the second CO ligand is eventually substituted, resulting in a ^{31}P NMR spectrum that is characteristic of a square planar complex albeit with large coupling constants between the phosphorus atoms (see Table 4). This coupling constant is relatively high for a complex with the phosphorus ligands oriented in a cis fashion. The only reference we are aware of presents a lower value (70 Hz).[22] The IR spectrum shows no CO absorptions (complex **B**).

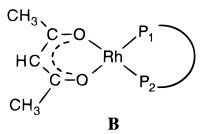

B

For complex RhAcac(**4**), an X-ray structure was determined (Figure 4; Tables 5, 6). The figure shows a square planar surrounded rhodium. The P(1)−Rh−P(2) angle of 97.5(1)° is large compared to the analogous triphenyl phosphite complex[23] (94.8(2)°) and demon-

(22) Aigen, S.; Van Eldik, R. *Organometallics* **1987**, *6*, 1080.
(23) Leipoldt, J. G.; Lamprecht, G. J.; Van Zyl, G. J. *Inorg. Chim. Acta* **1985**, *96*, 31.

Table 5. Crystallographic Data for RhAcac(4) and 11

	compound	
	Rh(acac)(**4**)	**11**
	Crystal Data	
formula	$C_{73}H_{95}Cl_2O_8P_2Rh\cdot1.5C_2H_5OH$	$C_{70}H_{89}Cl_2O_8P_2Rh$
M_n	1405.41	1294.23
cryst system	triclinic	monoclinic
space group	$P\bar{1}$ (No. 2)	$C2/c$ (No. 15)
a, Å	17.485(4)	40.632(6)
b, Å	18.838(2)	13.943(3)
c, Å	14.220(1)	23.645(5)
α, deg	110.16(1)	90
β, deg	107.97(1)	92.420(15)
γ, deg	87.98(1)	90
V, Å^3	4169(1)	13384(4)
D_{calc}, g cm^{-3}	1.12	1.29
Z	2	8
F(000)	1490	5456
μ cm^{-1}	30.3 (Cu Kα)	4.3 (Mo Kα)
cryst size, nm	0.15 × 0.40 × 0.45	0.50 × 0.25 × 0.15
	Data Collection	
T, K	250	150
θ_{SET4} range, deg	40−42	10.1−13.9
θ_{min}, θ_{max} deg	2.5, 65.5	1.5, 23.5
wavelength, Å	1.541 84 (graphite monochr)	0.710 73 (graphite monochr)
scan type	$\omega/2\theta$	ω
X-ray exposure time, h	172	28
linear decay, %	8	0
ref refln	$1\bar{1}0$, $01\bar{1}$	17 3 3, 6 4 11, 11 5 9
Data set	0:20, −22:22, −16:15	−45:45, 0:15, 0:26
tot. no. of data	14 136	10 633
tot. unique data	14 136	9873
DIFABS transm range	0.62−1.67	0.834−1.180
	Refinement	
no. of refined params	1066	773
final R1[a] [no. of data]	0.087 [9433, $I > 2.5\sigma$(I)]	0.082 [4807, $F_o > 4\sigma(F_o)$]
final wR2[b] [no. of data]		0.164 [9873]
final R_w[c] [no. of data]	0.116 [9433]	
S	1.04	0.935
ω^{-1} [d]	$[6.2 + 0.0129(\sigma(R_o))^2 + 0.0002/(\sigma(R_o))]$	$\sigma^2(F^2) + (0.0509P)^2$
$(\Delta/\sigma)_{av}$, $(\Delta/\sigma)_{max}$	0.04, 0.95	0.008, 0.742
min and max residual density, e Å^{-3}	−1.4, 1.3	−0.62, 0.52

[a] $R1 = \sum||F_o| - |F_c||/\sum|F_o|$. [b] $wR2 = [\sum[w(F_o^2 - F_c^2)^2]/\sum[w(F_o^2)^2]]^{1/2}$. [c] $R_w = [\sum[w(||F_o| - |F_c||)^2]/\sum[w(F_o^2)]]^{1/2}$. [d] $P = (\max(F_o^2, 0) + 2F_c^2)/3$.

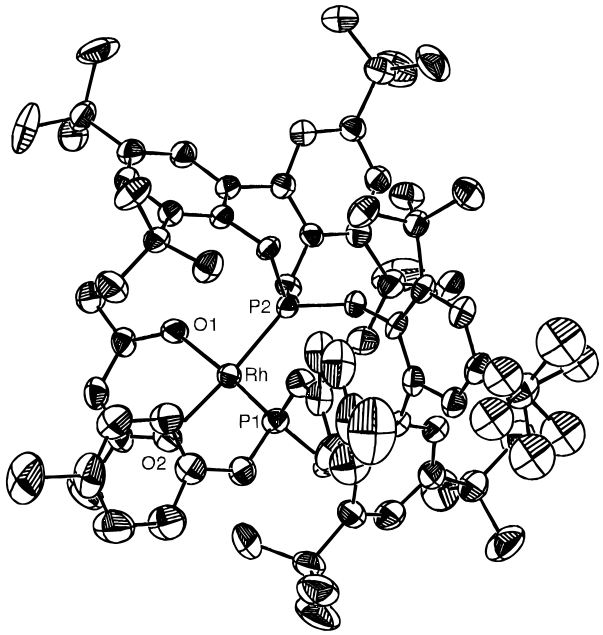

Figure 4. ORTEP plot of RhAcac(**4**) at the 50% probability level. Hydrogen atoms and the minor disorder contribution were left out for clarity.

strates the steric hindrance of the diphosphite. This enlarged P−Rh−P angle was previously observed for

Table 6. Selected Bond Lengths (Å) and Bond Angles (deg) of RhAcac(4) (Esd's in Parentheses)

	Distances		
Rh−P(1)	2.134(3)	Rh−O(1)	2.053(8)
Rh−P(2)	2.170(3)	Rh−O(2)	2.056(8)
	Angles		
P(1)−Rh−P(2)	97.5(1)	Rh−P(2)−O(7)	109.7(3)
P(1)−Rh−O(1)	171.5(2)	Rh−P(2)−O(8)	114.1(2)
P(1)−Rh−O(2)	88.8(3)	O(6)−P(2)−O(7)	98.7(4)
P(2)−Rh−O(1)	86.6(2)	O(6)−P(2)−O(8)	99.2(4)
P(2)−Rh−O(2)	173.8(3)	O(7)−P(2)−O(8)	102.0(4)
O(1)−Rh−O(2)	87.2(3)	P(1)−O(3)−C(6)	129.1(8)
Rh−P(1)−O(3)	117.0(3)	P(1)−O(4)−C(12)	130.3(9)
Rh−P(1)−O(4)	115.0(3)	P(1)−O(5)−C(18)	124.9(7)
Rh−P(1)−O(5)	124.1(3)	P(2)−O(6)−C(32)	140.8(6)
O(3)−P(1)−O(4)	103.0(5)	P(2)−O(7)−C(46)	123.4(8)
O(3)−P(1)−O(5)	90.8(4)	P(2)−O(8)−C(60)	119.9(8)
O(4)−P(1)−O(5)	102.8(5)	Rh−O(1)−C(1)	129.2(7)
Rh−P(2)−O(6)	129.3(3)	Rh−O(2)−C(3)	125.8(8)

RhAcacP_2, where P_2 = bis(phenyl 3,3′,5,5′-tetra-*tert*-butyl-1′,1′-biphenyl-2,2′-diyl phosphite) (99.87(3)°).[24] The Rh−P distances (2.1549(9) and 2.1566(9) Å) and the Rh−O distances (2.070(2) and 2.074(2) Å) in the above mentioned bis(phosphite)-derived complex are similar to those in RhAcac(**4**) (Rh−P(1) = 2.134(3) and 2.170(3) Å, Rh−O(1) = 2.053(8), Rh−O(2) = 2.056(8)). The

(24) Jongsma, T.; Challa, G.; Van Leeuwen, P. W. N. M. *J. Organomet. Chem.* **1991**, *421*, 121. Meetsma, A.; Jongsma, T.; Challa, G.; Van Leeuwen, P. W. N. M. *Acta Crystallogr.* **1993**, *C49*, 1160.

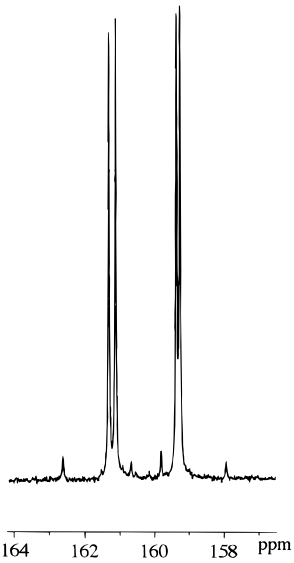

Figure 5. $^{31}P[^{1}H]$ NMR spectrum (300 MHz, benzene-d_6) of product formed after pressurizing ($P_{CO/H_2} = 10$ bar) and heating ($T = 60$ °C) $Rh(CO)_2Acac$ + **4**.

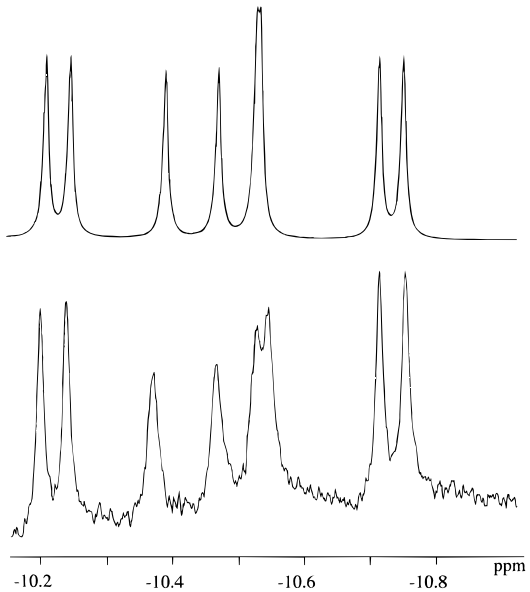

Figure 6. Hydride region of measured ^{1}H NMR spectrum (100 MHz, benzene-d_6, lower) and simulated spectrum (upper) of product formed after pressurizing ($P_{CO/H_2} = 10$ bar) and heating ($T = 60$ °C) $Rh(CO)_2Acac$ + **4**.

O(1)−Rh−O(2) angle of 87.2(3)° is somewhat smaller than that in the $RhAcacP_2$ complex (89.41(9)°) and in the triphenyl phosphite analogue (88.8(2)°). The distortion is also noticeable from the various, very large P−O−C angles that are present. A molecular mechanics study of P−O−C angles of $Cr(CO)_5L$ complexes (with L = phosphite)[25] revealed that the average angles in the chromium complex are larger than in the free ligand. They increase with increasing bulkiness of the phosphite with a maximum of 127.5° for $L = P(O\text{-}t\text{-}Bu)_3$. In RhAcac(**4**) a very large angle of 140.8(6)° was determined for P(2)−O(6)−C(32), possibly meaning that steric hindrance has led to distortions within the diphosphite. Triphenylphosphine exclusively yields monophosphine complexes when reacted with $Rh(Acac)(CO)_2$, even when a large excess of phosphine is used.[26] The chelating effect on coordination of the two phosphorus atoms and the high π-acidity, leading to formation of strong coordination bonds, might explain that the complex is formed despite the large steric hindrance of the diphosphite. It also clarifies the extreme conditions required to substitute the second CO ligand of $Rh(CO)_2Acac$. One of the *tert*-butyl groups is disordered (C(38)−C(41).

The symmetric diphosphites give rise to chelating coordination immediately upon mixing or after stirring for several minutes. For some of the diphosphites a side product is obtained that has both phosphorus atoms coordinated to the rhodium center and that still shows a CO vibration. These types of complexes, containing a 5-coordinated rhodium center, were previously described by Buisman *et al.*[7c,d]

When performing the same experiment under syngas pressure (in a high-pressure NMR tube, $P = 12$ bar, 1:1 CO/H_2), we also see formation of **A**, but after heating of the mixture, a complex of type **B** is not observed; the ^{31}P-NMR spectrum now shows two ^{31}P signals with two different Rh−P coupling constants (243, 226 Hz) indicative of two coordinating phosphorus atoms (see Figure 5) and a TBP surrounding of the rhodium. In the hydride region of the ^{1}H NMR a second-order multiplet is observed (Figure 6). Repeating this experiment with 5 equiv of **4** resulted in formation of a mixture of 1 equiv of the diphosphite complex and 4 equiv of the free ligand.

We followed this reaction with *in-situ* infrared spectroscopy. After mixing of the diphosphite with the $Rh(CO)_2Acac$ precursor, instantaneously **A** was observed. After pressurization of the mixture with 10 bar of syngas, a large amount of $Rh(CO)_2Acac$ was re-formed, of which the CO vibrations disappeared on the appearance of two new vibrations in the carbonyl region. These IR and NMR data point toward a five-coordinated Rh(I) complex as the final complex containing a hydrido ligand and the diphosphite coordinated in a bidentate way. The reported formation of dimeric bimetallic species at higher temperatures[11] was not observed under our conditions. No infrared signals in the bridging CO region (1800−1900 cm^{-1}) could be detected, and both ^{31}P and ^{1}H NMR showed only the signals that could be assigned to the monomeric rhodium hydride complex.

The active catalyst complex that appeared to be quite air stable was prepared in the autoclave (see Experimental Section) and was characterized under air. Complexes with the other diphosphites were prepared in this way, and the obtained spectroscopic data are shown in Tables 7 and 8. For some of the hydridorhodium complexes ^{103}Rh NMR was measured as well, and these data confirmed that each Rh center is coordinated to two phosphorus atoms.

Hydridorhodium Complexes of Nonsymmetric Diphosphites. Simulation of the NMR data showed that the complicated spectra obtained with the nonsymmetric diphosphites **1**−**5** are caused by two phosphorus atoms that have accidentally almost equal chemical shifts, although they are chemically inequivalent. They show different hydrogen−phosphorus coupling constants which are in the same order of magnitude as the difference in the phosphorus chemical shift values. The values of the ^{31}P chemical shifts point toward an ee coordination of the diphosphite ligand, but the hydrogen−phosphorus coupling constants resemble neither a cis

(25) Caffrey, M. L.; Brown, T. L. *Inorg. Chem.* **1991**, *30*, 3907.
(26) Bonati, F.; Wilkinson, G. *J. Chem. Soc. A* **1964**, 3156.

Table 7. NMR Data (300.12 MHz) for $RhH(CO)_2$(diphosphite) (Benzene-d_6) Obtained after Simulation (GeNMR)

diphosphite	$\delta(^{31}P)$ (ppm)	$\delta(^{1}H)$ (ppm)	$\delta(^{13}C)$ (ppm)	$\delta(^{103}Rh)$ (ppm)	coupling consts (Hz)
1	160.6	−10.35		−1073	$J_{RhP1} = 240$, $J_{RhP2} = 233$, $J_{PP} = 250$, $J_{HP1} = -70$, $J_{HP2} = 23$, $J_{RhH} = 3$
1 (^{13}CO complex)	160.8, 160.6	−10.31	193.7, 191.9		$J_{RhP1} = 230$, $J_{RhP2} = 234$, $J_{PP} = 250$, $J_{HP1} = -73$, $J_{HP2} = 18$, $J_{RhH} = 2.5$, $\lvert J_{PC1}\rvert = 8$, $\lvert J_{PC2}\rvert = 42$, $J_{RhC1} = 53$, $J_{RhC2} = 67.5$
2[a]	156.0, 155.7				$J_{RhP1} = 234$, $J_{RhP2} = 228$, $J_{PP} = 250$, $J_{HP1} = -50$, $J_{HP2} = 96$, $J_{RhH} = 3$
3[a]	160.9, 160.7	−10.58		−1070	$J_{RhP1} = 235$, $J_{RhP2} = 222$, $J_{PP} = 225$, $J_{HP1} = -45$, $J_{HP2} = 93$, $J_{RhH} = 3$
4	160.5, 159.8	−10.40		−1070	$J_{RhP1} = 237$, $J_{RhP2} = 226$, $J_{PP} = 170$, $J_{HP1} = -19$, $J_{HP2} = 70$, $J_{RhH} = 3.5$
4 (^{13}CO complex)	160.5, 159.8	−10.40	193.5, 191.9		$J_{RhP1} = 237$, $J_{RhP2} = 226$, $J_{PP} = 170$, $J_{P1C1} = -2.5$, $J_{P1C2} = 47$, $J_{P2C1} = 14$, $J_{P2C2} = 38$, $J_{RhCl} = 54$, $J_{RhC2} = -65$
5[b]	162.5, 161.2	−10.61			$J_{RhP1} = 211$, $J_{RhP2} = 235$, $J_{PP} = 115$, $J_{HP1} = 82$, $J_{HP2} = -10$, $J_{RhH} = 3$
6	161.3	−9.72			$J_{RhP} = 213$, $J_{PH} = 72$, $J_{RhH} = 6.5$
7	171.0	−9.80			$J_{RhP} = 226$, $J_{PH} = 5$, $J_{RhH} = 3.5$
8	174.5	−10.81	194.7		$J_{RhP} = 239$, $J_{PH} = 4$, $J_{RhH} = 3.5$
9	173.0	−10.30			$J_{RhP} = 234$, $J_{PH} = 9$, $J_{RhH} = 3$
10	151.6	−10.97			$J_{RhP} = 244$, $J_{PH} = 4$, $J_{RhH} = 5$

[a] Toluene-d_8. [b] Acetone-d_6.

Table 8. IR Frequencies in the M−H and CO Stretching Region of Hydridorhodium Diphosphite Complexes

diphosphite	ν (cm^{-1})
1	2033, 1995[a]
	2030, 1994, 1988[b]
	1988, 1949[c] (^{13}CO complex)
2	2031, 1992[a]
3	2031, 1990[c]
4	2049, 1966[a]
	2035, 1998, 1990[b]
	2058, 2012[b] (deuteride complex)
	1994, 1957[c] (^{13}CO complex)
5	2028, 1998[a]
6	2028, 1987[a]
8	2074, 2013[a]
10	2070, 2008[a]

[a] In acetone-d_6. [b] As a Nujol mull. [c] In benzene-d_6.

nor a trans relation of the phosphorus atoms toward the hydrido ligand.[27] In Table 7 it is also shown that, going from **1** and **5**, the difference in the chemical shift between the phosphorus atoms increases. For **1** and **4** we have prepared the catalyst complexes with ^{13}CO. The HRh(**1**)(^{13}CO)$_2$ spectrum shows two virtual double triplets in the carbonyl region. $J_{RhC1} = 53$ Hz and $J_{RhC2} = 67.5$ Hz ($\lvert J_{PC1}\rvert = 8$ Hz, $\lvert J_{PC2}\rvert = 42$ Hz). From the ^{31}P NMR data it was concluded that, in this ligand, of all nonsymmetric ones, the phosphorus atoms have the smallest difference in chemical shift (<0.1 ppm). Thus, the two phosphorus−carbon coupling constants give rise to virtual triplets. On the contrary, HRh(**4**)(^{13}CO)$_2$ shows a first-order ^{13}C spectrum with two different CO ligands coupled by two unidentical phosphorus atoms. In the simulated ^{31}P NMR spectrum the difference in chemical shift is 0.7 ppm. From these data it becomes clear that in these complexes the CO ligands do not exchange their positions. Most likely, on the NMR time scale the phosphorus ligands retain their positions as well.

IR spectra of the complexes that could be obtained as powders were measured as Nujol mulls (see for IR data Table 8). It was found that three absorptions were present in the CO-stretching region instead of two observed with IR in solution. Upon measurement of DRh(CO)$_2$(**4**), only two absorptions remained (2058, 2012 cm^{-1}), which were shifted compared to HRh(CO)$_2$(**4**) (2035, 1998, 1990 cm^{-1}). This implies that the three frequencies in the hydrido complex are combinations of two CO ligands and one hydrido ligand. The rhodium−hydride vibration disappears upon deuterating the complex as the rhodium−deuteride vibration is situated in the fingerprint region. The large frequency shift of the highest energy absorption is indicative of a trans hydrido−CO relation.[28] In solution IR, the rhodium hydride vibration and the lowest energy CO vibration overlap resulting in two absorptions. Combining the spectroscopic experiments, we can conclude that the catalyst complex contains a chelating diphosphite, a hydrido ligand, and two CO ligands coordinated to the rhodium center. Although the coupling constants of the phosphorus atoms with the hydrido ligand do not lead to straightforward conclusions, from IR spectroscopy and the nearly identical ^{31}P chemical shifts and phosphorus−rhodium coupling constants, which indicated two nearly identical phosphorus atoms, we assume that the diphosphite is bisequatorially coordinated (ee) and the complex has structure **C**.

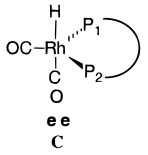

C

This structure is confirmed by the X-ray determination of HRh(CO)$_2$(**4**)[29] (**11**) (Tables 5, 9, 10; Figure 7). The crystal structure shows a distorted TBP geometry around the rhodium with both the phosphorus atoms in equatorial positions. The P(1)−Rh−P(2) angle is 115.95(9)°. The hydrido ligand could not be found. One CO ligand is situated equatorially, and the other CO molecule and the hydrido ligand occupy axial positions. The angles of the phosphorus atoms with the axial CO are 92.1(3)° for P(1)−Rh−C and 104.2(3)° for P(2)−Rh−C, meaning that CO(ax) deviates from the molecular axis. The rhodium atom is situated out of the equatorial plane (0.395(1) Å), having moved somewhat toward the axial CO ligand. This distortion explains the relatively high hydrogen−phosphorus coupling constants that were determined by simulation of the NMR spectra; apparently the H−Rh−P angles are larger than 90° resulting in larger coupling constants than expected for

(27) Hyde, E. M.; Swain, J. R.; Verkade, J. G.; Meakin, P. *J. Chem. Soc., Dalton Trans.* **1976**, 1169.

(28) Vaska, L. *J. Am. Chem. Soc.* **1966**, *88*, 4100.

(29) Van Rooy, A.; Kamer, P. C. J.; Van Leeuwen, P. W. N. M.; Veldman, N.; Spek, A. L. *J. Organomet. Chem.* **1995**, *494*, C15.

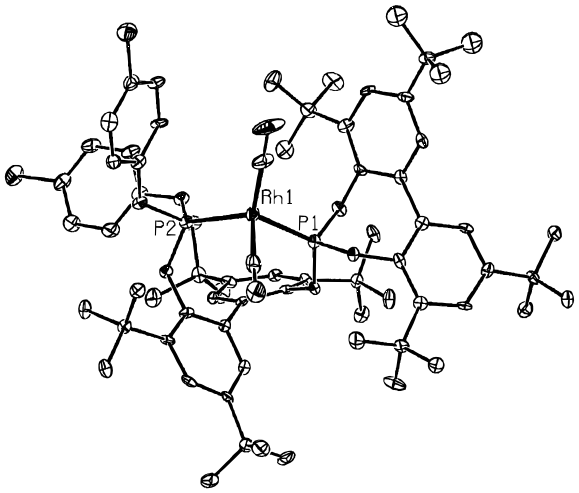

Figure 7. ORTEP plot of **11** at the 30% probability level. Hydrogen atoms and the minor disorder contribution were left out for clarity.

Table 9. Selected Bond Lengths (Å) and Bond Angles (deg) of 11 (Esd's in Parentheses)

		Distances	
Rh−P(1)	2.255(3)	Rh−C(69)	1.878(12)
Rh−P(2)	2.239(3)	Rh−C(70)	1.938(9)
		Angles	
P(1)−Rh−P(2)	115.95(9)	Rh−P(2)−O(5)	119.3(2)
P(1)−Rh−C(69)	115.2(4)	Rh−P(2)−O(6)	117.5(2)
P(2)−Rh−C(69)	118.5(3)	O(4)−P(2)−O(5)	94.6(3)
P(1)−Rh−C(70)	92.1(3)	O(4)−P(2)−O(6)	101.5(3)
P(2)−Rh−C(70)	104.2(3)	O(5)−P(2)−O(6)	99.3(3)
C(69)−Rh−C(70)	105.8(4)	P(1)−O(1)−C(1)	117.3(5)
Rh−P(1)−O(1)	118.1(2)	P(1)−O(2)−C(12)	123.0(4)
Rh−P(1)−O(2)	110.4(2)	P(1)−O(3)−C(29)	117.9(5)
Rh−P(1)−O(3)	124.2(2)	P(2)−O(4)−C(40)	126.5(5)
O(1)−P(1)−O(2)	104.6(3)	P(2)−O(5)−C(57)	123.1(5)
O(1)−P(1)−O(3)	97.8(3)	P(2)−O(6)−C(63)	124.7(5)
O(2)−P(1)−O(3)	98.6(3)	Rh(1)−C(69)−O(8)	174.2(9)
Rh−P(2)−O(4)	120.2(2)	Rh(1)−C(70)−O(7)	176.4(8)

a complex with the phosphites in a pure cis arrangement. Alternatively, the complex can be seen as having a distorted tetrahedral geometry with the hydrido ligand on one of the faces. The Rh−C−O angles show a slight deviation from 180° (174.2 and 176.4°). The dihedral angles of the diphenyl rings are 60.6(4)° for C(29)−C(34) with C(35)−C(40) and 61.9(4)° for C(1)−C(6) with C(7)−C(12), respectively. One of the *tert*-butyl substituents (C(17), C(18), C(19), C(20)) is disordered.

This is the first crystal structure of a hydridorhodium diphosphite complex reported to our knowledge. In the square planar complex derived from **4**, RhAcac(**4**), the Rh−P distances (2.134(3) and 2.170(3) Å) are shorter than those in **11** (2.239(3) and 2.255(3) Å).

The crystal structure of **11** shows much similarities with those of the recently crystallographically analyzed Ir(BISBI)$(CO)_2$H and HRh(CO)(PPh_3)(BISBI) (BISBI = 2,2′-bis(diphenylphosphinomethyl)(1,1′-biphenyl)) reported by Casey *et al.*[2a] Except for the oxygen *vs* carbon atom, BISBI and **4** have similar bridges between both phosphorus atoms. The hydroformylation of hex-1-ene with the rhodium catalyst derived from BISBI yields a normal to branched ratio of 50, which was also ascribed to bisequatorial coordination of the diphosphine according to the authors. The Rh−P distances (2.285(1) and 2.318(1) Å) of HRh(CO)(PPh_3)(BISBI) are similar to the Rh−P distances (2.239(3) and 2.255(3) Å) of **11**, and the P−Rh−P angle is 124.8(1)°, which is larger than that of **11**, despite the sterically more demanding and also equatorially coordinating triphenylphosphine ligand. In the Ir complex the P−Ir−P angle is 117.9(1)°, more similar to the P−Rh−P angle of **11**. Complex **11** has a more distorted structure than the BISBI compounds indicative of more steric crowding.

The ee coordination of BISBI to the rhodium follows from a natural bite angle of approximately 120°. In order to obtain high regioselectivities ee coordination and hence a 120° bite angle is required. The structure of **11** confirms this suggestion.

Hydridorhodium Complexes of Symmetric Diphosphites. The symmetric diphosphites **6**−**9** all give rise to hydridorhodium complexes that show clear first-order spectra in which the phosphorus atoms are equivalent on the NMR time scale at room temperature. The hydridorhodium complexes derived from **7**−**9** show very small P−H coupling constants (4−9 Hz) indicative of ee-coordinated complexes. On cooling of HRh$(CO)_2$(**8**), the phosphorus atoms lose their time averaged equivalence, and at T = 205 K the slow exchange situation is reached, resulting in a strongly coupled NMR spectrum (^{31}P NMR δ (ppm) 177.3, 175.4, J_{RhP1} = 238, J_{RhP2} = 232, J_{PP} = 205 Hz (acetone-d_6)). However, the P−H coupling constant remains small (not detectable as a consequence of broadening of signals at low temperatures). The existence of two inequivalent phosphorus atoms can be explained by hindered rotation of the bridge between the phosphorus atoms. The two aromatic rings can rotate freely at higher temperatures, which results in two equivalent phosphorus atoms. At low temperatures this process is slowed down and the two P's become inequivalent on the NMR time scale. The room-temperature ^{13}C NMR spectrum of the ^{13}CO derived hydridorhodium complex of **8** gives rise to a double triplet in accordance with two equivalent phosphorus atoms and two equivalent CO ligands meaning that here the CO ligands are in fast exchange.

The hydridorhodium complex of diphosphite **7** does not form easily, and the precursor requires 8 h instead of 3 h under syngas pressure. Diphosphite **6** forms the HRh$(CO)_2$(**6**) complex very slowly as well (8 h required), and the reaction is accompanied with much decomposition as is shown by signals at ≈10 ppm in the ^{31}P NMR, originating from H-phosphonates formed by hydrolysis. The structure of this hydrido complex is different, because, in this complex, the phosphorus atoms are equatorially axially (ea) coordinated as was concluded from NMR at low temperatures. At room temperature the phosphorus atoms are in fast exchange resulting in one doublet caused by the coupling with the rhodium center. The ^{1}H NMR hydride region contains a virtual double triplet with a phosphorus hydride coupling constant of 72 Hz. We were not able to reach the slow-exchange region by cooling, but in the ^{1}H NMR at 200 K we did observe a broad doublet (J_{PH} = 180 Hz; the signal is too broad to observe other couplings, $\Delta\nu_{1/2}$ = 15 Hz) indicative of a trans relation of one phosphorus atom toward the hydrido ligand. We reacted HRh(CO)-$(PPh_3)_3$ with **6** in order to prepare a more stable hydrido−rhodium complex,[2a] HRh(CO)(PPh_3)(**6**) (see Experimental Section). Indeed a stable complex was obtained, and from the coupling constants of the hydrido ligand of **6** with the phosphorus atom from the PPh_3 ligand (13 Hz) and different couplings constant of the

Table 10. Final Atomic Coordinates and Equivalent Isotropic Thermal Parameters (Å²) for 11 (Esd's in Parentheses)[a]

atom	*x*	*y*	*z*	*U*(eq)	atom	*x*	*y*	*z*	*U*(eq)
Rh(1)	0.17325(2)	0.18205(5)	0.19841(3)	0.0312(3)	C(28)	0.0988(2)	0.0361(6)	0.3337(4)	0.043(3)
Cl(1)	0.16020(6)	0.6768(2)	−0.05226(10)	0.0538(12)	C(29)	0.0800(2)	0.1750(6)	0.1424(3)	0.018(2)
Cl(2)	0.33688(5)	0.3179(2)	0.15785(12)	0.0556(10)	C(30)	0.0633(2)	0.1387(5)	0.0936(3)	0.021(3)
P(1)	0.13069(5)	0.0797(2)	0.18458(9)	0.0211(7)	C(31)	0.0576(2)	0.2050(5)	0.0512(3)	0.023(3)
P(2)	0.16663(5)	0.3279(2)	0.15996(9)	0.0239(7)	C(32)	0.0645(2)	0.3019(6)	0.0547(3)	0.024(3)
O(1)	0.12871(13)	0.0176(4)	0.1266(2)	0.0248(17)	C(33)	0.0763(2)	0.3351(5)	0.1074(3)	0.019(2)
O(2)	0.13078(12)	0.0015(4)	0.2339(2)	0.0211(17)	C(34)	0.0844(2)	0.2717(5)	0.1521(3)	0.016(2)
O(3)	0.09210(12)	0.1109(3)	0.1851(2)	0.0175(17)	C(35)	0.0915(2)	0.3130(6)	0.2097(3)	0.017(2)
O(4)	0.13918(12)	0.3985(4)	0.1819(2)	0.0217(17)	C(36)	0.0690(2)	0.2944(5)	0.2507(3)	0.019(3)
O(5)	0.19644(12)	0.4062(4)	0.1671(2)	0.0260(17)	C(37)	0.0701(2)	0.3396(5)	0.3035(3)	0.022(3)
O(6)	0.15983(12)	0.3340(4)	0.0918(2)	0.0256(17)	C(38)	0.959(2)	0.4043(5)	0.3131(3)	0.022(3)
O(7)	0.1584(2)	0.2064(5)	0.3236(3)	0.054(3)	C(39)	0.1195(2)	0.4266(6)	0.2751(3)	0.022(3)
O(8)	0.2407(2)	0.0909(7)	0.1943(4)	0.107(4)	C(40)	0.1166(2)	0.3785(6)	0.2234(3)	0.021(3)
C(1)	0.1534(2)	−0.0502(6)	0.1192(3)	0.022(3)	C(41)	0.0477(2)	0.0389(6)	0.0845(4)	0.026(3)
C(2)	0.1765(2)	−0.0439(6)	0.0780(3)	0.028(3)	C(42)	0.0467(2)	−0.0228(6)	0.1383(4)	0.034(3)
C(3)	0.2014(2)	−0.1116(6)	0.0796(4)	0.030(3)	C(43)	0.0647(2)	−0.0183(6)	0.0395(4)	0.036(3)
C(4)	0.2026(2)	−0.1900(6)	0.1178(4)	0.030(3)	C(44)	0.0112(2)	0.0559(6)	0.0661(3)	0.032(3)
C(5)	0.1767(2)	−0.1991(6)	0.1522(4)	0.027(3)	C(45)	0.0567(2)	0.3666(6)	0.0033(3)	0.026(3)
C(6)	0.1518(2)	−0.1316(5)	0.1536(3)	0.020(2)	C(46)	0.0243(2)	0.3405(6)	−0.0262(4)	0.041(3)
C(7)	0.1226(2)	−0.1490(6)	0.1885(4)	0.026(3)	C(47)	0.0849(2)	0.3528(6)	−0.0376(3)	0.039(3)
C(8)	0.1043(2)	−0.2309(6)	0.1779(3)	0.019(3)	C(48)	0.0549(2)	0.4709(6)	0.0199(4)	0.043(3)
C(9)	0.0766(2)	−0.2513(6)	0.2081(3)	0.025(3)	C(49)	0.0444(2)	0.3262(6)	0.3484(3)	0.028(3)
C(10)	0.0696(2)	−0.1879(6)	0.2512(3)	0.022(3)	C(50)	0.0286(2)	0.4232(6)	0.3599(4)	0.042(3)
C(11)	0.0871(2)	−0.1046(6)	0.2644(3)	0.022(2)	C(51)	0.0167(2)	0.2583(7)	0.3294(4)	0.045(3)
C(12)	0.1129(2)	−0.0853(5)	0.2294(3)	0.021(3)	C(52)	0.0606(2)	0.2895(6)	0.4031(4)	0.047(3)
C(13)	0.1776(2)	0.0293(6)	0.0276(4)	0.039(3)	C(53)	0.1472(2)	0.4999(6)	0.2907(3)	0.024(3)
C(14)	0.1500(2)	0.1041(6)	0.0262(4)	0.046(3)	C(54)	0.1795(2)	0.4464(6)	0.3040(4)	0.033(3)
C(15)	0.2107(2)	0.0814(7)	0.0292(4)	0.055(4)	C(55)	0.1382(2)	0.5566(6)	0.3436(4)	0.034(3)
C(16)	0.1737(3)	−0.0296(7)	−0.0266(3)	0.052(4)	C(56)	0.1521(2)	0.5739(6)	0.2448(4)	0.036(3)
C(17)	0.2310(2)	−0.2596(6)	0.1209(4)	0.030(3)	C(57)	0.2296(2)	0.3820(6)	0.1636(4)	0.027(3)
C(18A)*	0.2631(3)	−0.2233(13)	0.0972(8)	0.064(6)	C(58)	0.2511(2)	0.4241(6)	0.2017(4)	0.035(3)
C(18B)*	0.2617(5)	−0.2011(17)	0.1398(13)	0.061(9)	C(59)	0.2841(2)	0.4058(7)	0.1996(4)	0.040(3)
C(19A)*	0.2407(4)	−0.2860(13)	0.1834(5)	0.063(6)	C(60)	0.2954(2)	0.3431(6)	0.1599(4)	0.037(3)
C(19B)*	0.2362(6)	−0.2989(19)	0.0606(7)	0.058(9)	C(61)	0.2738(2)	0.3001(6)	0.1214(4)	0.032(3)
C(20A)*	0.2216(4)	−0.3537(10)	0.0915(8)	0.066(7)	C(62)	0.2403(2)	0.3212(7)	0.1231(3)	0.031(3)
C(20B)*	0.2257(7)	−0.3457(16)	0.1600(12)	0.077(11)	C(63)	0.1605(2)	0.4194(6)	0.0598(4)	0.028(3)
C(21)	0.0536(2)	−0.3340(5)	0.1927(4)	0.025(3)	C(64)	0.1432(2)	0.4994(6)	0.0741(4)	0.039(3)
C(22)	0.0671(2)	−0.3986(6)	0.1470(4)	0.040(3)	C(65)	0.1435(2)	0.5782(7)	0.0386(4)	0.041(3)
C(23)	0.0489(2)	−0.3969(6)	0.2449(4)	0.036(3)	C(66)	0.1611(2)	0.5771(7)	−0.0085(4)	0.040(3)
C(24)	0.0204(2)	−0.2929(6)	0.1714(4)	0.035(3)	C(67)	0.1792(2)	0.4975(7)	−0.0220(4)	0.041(3)
C(25)	0.0760(2)	−0.0461(6)	0.3143(3)	0.029(3)	C(68)	0.1790(2)	0.4170(7)	0.0129(4)	0.034(3)
C(26)	0.0733(2)	−0.1112(6)	0.3658(3)	0.041(3)	C(69)	0.2152(3)	0.1255(8)	0.1989(4)	0.056(4)
C(27)	0.0411(2)	−0.0045(7)	0.3006(4)	0.49(4)	C(70)	0.1635(2)	0.2004(7)	0.2772(4)	0.043(3)

[a] *U*(eq) = $^1/_3$ of the trace of the orthogonalized *U*. Starred atom sites have a population less than 1.0.

hydrido with the phosphorus atoms of **6** (−191 and 13 Hz) it became clear that also in this complex diphosphite **6** is ea coordinated. Likewise, in $HRh(CO)(PPh_3)$(**4**) the diphosphite was found to coordinate in an ee way as in the dicarbonyl complexes (small hydrogen−phosphorus coupling constants: 20, 9, 4 Hz).

It appears that at room temperature in the ee-coordinated complexes of the nonsymmetric diphosphites the phosphorus atoms and the CO ligands retain their positions in the TBP surrounding rhodium (on the NMR time scale), while the ea complexes easily undergo structural isomerization, as in the $HRh(CO)_2$(**6**) compound and several analogous complexes published by Buisman.[7c,d] From his work it was concluded that ligands with a preference for ea coordination always lead to more fluxional complexes than those leading to ee coordination, even if these ea ligands are more rigid; ea diphosphite complexes are intrinsically more fluxional. This can be explained by the flexibility of the ligands, *i.e.* the feasible P−Rh−P angles, upon coordination.

Isomerization can occur via two mechanisms. The pseudo Berry rotation[30] requires a square-pyramidal structure as intermediate. Meakin[31] described an exchange process which involves a tetrahedral surrounding of the metal. The flexible ea-coordinating diphosphites may be able to coordinate with varying P−Rh−P angles, giving rise to fast exchange, while the diphosphites with rigid biphenyl backbones show less flexibility.

Structure−Selectivity Relationships. In this last section we will try to explain the catalyst behavior in relation to the structural information obtained. First we have to ascertain that under the highly diluted conditions of the catalytic experiments the same hydrido species are formed that we observed with NMR and IR spectroscopy. From the work of Jongsma[32] on the bulky monophosphite tris(2-*tert*-butyl-4-methylphenyl) phos-

(30) Berry, R. S. *J. Chem. Phys.* **1960**, *32*, 933.

(31) Meakin, P.; Muetterties, E. L.; Jesson, J. P. *J. Am. Chem. Soc.* **1972**, *94*, 5271.

(32) Jongsma, T. Ph.D. Thesis, Rijksuniversiteit Groningen, 1992; Chapter 6.

(33) (a) Beurskens, P. T.; Admiraal, G.; Beurskens, G.; Bosman, W. P.; Gelder, R de; Israël, R.; Smits, J. M. M. *The DIRDIF-94 program system*; Crystallography Laboratory, University of Nijmegen: Nijmegen, The Netherlands, 1994. (b) Beurskens, P. T.; Admiraal, G.; Beurskens, G.; Bosman, W. P.; García-Granda, S.; Gould, R. O.; Smits, J. M. M.; Smykalla, C. *The DIRDIF program system*; Technical report of the Crystallography Laboratory; University of Nijmegen: Nijmegen, The Netherlands, 1992.

Scheme 2. Proposed Equilibrium for the Catalyst Precursors at High CO/H_2 Pressures

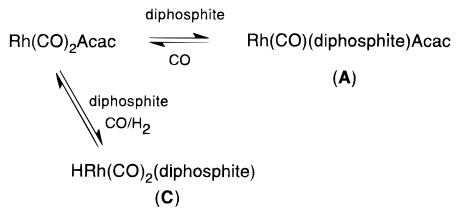

phite and the present results we learned that the equilibria in Scheme 2 exist in the catalyst system. Although neither **A** nor **B** has been detected during the formation of the active catalyst, Jongsma found that a 10-fold amount of bulky phosphite tris(2-*tert*-butylphenyl) phosphite was required to reach a total conversion of Rh(COD)Acac to the active complex $HRh(CO)_3P$ (P = tris(2-*tert*-butylphenyl) phosphite) although only one phosphorus ligand can coordinate to the rhodium center. The results of our *in-situ* infrared study are comparable to those of Jongsma,[32] and therefore, we also added a 10-fold amount of diphosphite to be certain that the same species is formed. Further addition of diphosphites does not increase the rate any further, and we conclude that all rhodium is converted to $HRh(CO)_2$-(diphosphite) (results not shown).

We conclude from the X-ray structure of $HRh(CO)_2$-(**4**) that the metal center is very crowded. As a consequence, there is little space for the incoming substrate. Unsubstituted 1-alkenes are the least sterically hindered and add to the metal most easily, followed by respectively 2-substituted 1-alkenes and internal alkenes. Upon migration of the hydride the steric interactions can be most efficiently diminished by the formation of a linear alkyl−rhodium intermediate. From the present results we cannot distinguish whether π-coordination or hydride migration or a combination thereof determines the regioselectivity, but the overall result remains the same. Viewed in that light we can understand our observations in both the hydroformylation of oct-1-ene and styrene. For oct-1-ene as the substrate a high product linearity will be obtained. For styrene, using the first type of ligands (**1**−**5**, **8**, **9**), ee coordinating and rigid, a reversed product selectivity, *viz*. an excess of linear phenylpropanal, can be obtained. The formation of the branched (1-phenylethyl)rhodium compound is now suppressed resulting in an increase in the formation of the linear aldehydes. At mild conditions the observed regioselectivity is low. This enlarged preference for 3-phenylpropanal can be exploited by the variation of reaction conditions. At higher temperatures and/or low CO pressures the rate of β-H elimination increases and eventually dominates the hydroformylation reaction. β-H elimination nearly exclusively occurs for the secondary (1-phenylethyl)-rhodium complex and prevents the formation of the branched aldehyde. The linear 2-phenylethyl, however, is almost irreversably formed and can complete the reaction cycle. Thus a higher *n*/*b* ratio is obtained.

In the second type of systems, in which an ea-coordinating (**6**) or a flexible (**7**) diphosphite is used, sufficient space is available for the substrate to form linear as well as branched alkylrhodium intermediates which results in high rates but low selectivities for oct-1-ene. These results are similar to those of the system containing DPPE which can only coordinate in an ea fashion.

Conclusions

In the hydroformylation of oct-1-ene the rhodium catalysts modified by the rigid diphosphites **1**−**5**, **8** and **9** give high rates and selectivities. The high regioselectivity is caused by steric repulsion of the diphosphites that coordinate bisequatorially to the rhodium center. The kinetics of the catalyst derived from $Rh(CO)_2Acac$ and **4** resemble those of the extensively studied PPh_3 system.[9] The flexible diphosphites **6** and **7** do not give satisfying results in the hydroformylation of oct-1-ene. Although rates are comparable with PPh_3 (the latter not added in large excess), the selectivity to normal aldehydes is moderate.

For styrene the selectivity can be directed to the formation of the linear or the branched aldehyde depending on the reaction conditions. The rigid diphosphites applied at high temperatures and low CO pressures give rise to a catalyst that forms the normal aldehydes in excess. When an ea-coordinating or a flexible diphosphite is used at low reaction temperatures, the catalyst favors formation of the branched 2-phenylpropanal.

Experimental Section

General Methods. All operations were performed under argon by standard Schlenk techniques. Solvents were distilled from sodium/benzophenone before use. NMR spectra were recorded on a Bruker AC-100 spectrometer (^1H, ^{103}Rh (measured via reverse 2D NMR) or a Bruker AMX-300 spectrometer (^1H, ^{13}C, ^{31}P, $^{31}P[^1H]$), and chemical shifts were reported referenced to tetramethylsilane and H_3PO_4, respectively. Infrared spectra were recorded on a Nicolet 510 FT-IR spectrophotometer. Mass spectroscopic data were obtained with the JEOL JMS SX/SX102A four-sector mass spectrometer, coupled to a JEOL MS-MP7000 data system. Gas−liquid chromatography analyses were done using a DB-1 column and a Carlo Erba GC 6000 Vega Series 2 chromatograph. The compounds **1**−**5** were prepared by a published method.[5a] $Rh(CO)_2$(pentane-2,4-dionate) was purchased from Johnson Matthey, triphenyl phosphite was purchased from Aldrich, and both were used as received. Column chromatography was performed with silica gel 60 230−400 mesh obtained from Merck. Syngas 3.0, CO 3.0, and H_2 5.0 were purchased from Praxair. Hydroformylation experiments were performed using $Rh(CO)_2$(pentane-2,4-dionate) and diphosphite as catalyst precursor in a stainless steel 316 autoclave, equipped with a magnetic stirring bar, a pressure transducer, a thermocouple, and a sampling device. Decane was used as the internal standard.

The autoclave, charged with solvent and catalyst precursor, was brought under pressure and heated to the reaction temperature. Upon addition of the substrate and the internal standard, the reaction started immediately. During the reaction, several samples were taken, quenched with $P(OPh_3)$ to deactivate the catalyst and analyzed by GLC.

The *in-situ* infrared experiment was performed in an SS 316 55 mL autoclave equipped with IRTRAN windows and a mechanical stirrer. $Rh(CO)_2Acac$ (10 mg, 3.88×10^{-6} mol) and **4** (0.042 g, 3.88×10^{-6} mol) were dissolved in 15 mL of cyclohexane. After pressurizing and heating of the mixture, the autoclave was placed in the infrared spectrometer, and while the samples were stirred, the infrared spectra were recorded.

Synthesis of Diphosphite Ligands. Preparation of 1,2-Bis(((4,4′,6,6′-tetra-*tert*-butyl-2,2′-bisphenoxy)phosphino)-oxy)ethane (6). A solution of PCl_3 (0.43 mL, 4.93 mmol), 4,4′,6,6′-tetra-*tert*-butyl-2,2′-bisphenol (2 g, 4.88 mmol) and triethylamine (1.4 mL, 10.10 mmol) in 40 mL of toluene was stirred for 2 h and additionally refluxed for 6 h. The mixture was filtered, and to the filtrate were added triethylamine (0.7 mL, 5.05 mmol) and ethane-1,2-diol (0.14 mL, 2.51 mmol). After being stirred for 12 h, the mixture was filtered and the solvent and excess of triethylamine were evaporated. The white compound was recrystallized from toluene/acetonitrile. Yield: 1.77 g of a white powder (1.89 mmol, 78%). $^{31}P[^1H]$ NMR: δ 134.7 ppm (s) ($CDCl_3$). ^1H NMR: δ (ppm) 7.41 (d, 4H arom, $J = 2.40$ Hz), 7.16 (d, 4H, arom, $J = 2.46$ Hz), 3.80 (d, 4H, C_2H_4, $J = 3.72$ Hz), 1.46 (s, 36H, *o*-C_4H_9), 1.34 (s, 36H, *p*-C_4H_9) ($CDCl_3$). Mp: 195−198 °C. Anal. Calcd for $C_{58}H_{84}O_6P_2$: C, 74.17; H, 9.02. Found: C, 73.95; H, 9.09.

Preparation of 1,3-Bis(((4,4′,6,6′-tetra-*tert*-butyl-2,2′-bisphenoxy)phosphino)oxy)propane (7). A solution of PCl_3 (0.6 mL, 7.40 mmol), 4,4′,6,6′-tetra-*tert*-butyl-2,2′-bisphenol (3 g, 7.32 mmol) and triethylamine (4 mL, 28.86 mmol) in 50 mL of toluene was stirred for 1 day. After filtration propane-1,3-diol (0.27 mL, 3.74 mmol) and triethylamine (2 mL, 14.43 mmol) were added and the reaction mixture was stirred overnight. The mixture was filtered and concentrated in vacuum. A crude product was obtained by crystallization from toluene/acetonitrile. The product was purified by column chromatography (eluent: 5% EtOAc/petroleum ether 60−80). Yield: 0.84 g (0.88 mmol, 24%). $^{31}P[^1H]$ NMR: δ (ppm) 136.2 (s) ($CDCl_3$). ^1H NMR: δ (ppm) 7.41 (d, 4H, arom, $J = 2.25$ Hz), 7.16 (d, 4H, arom, $J = 2.25$ Hz), 3.80 (m, 6H, C_3H_6), 1.46 (s, 36H, *o*-C_4H_9), 1.35 (s, 36H, *p*-C_4H_9) ($CDCl_3$). Mp: 152 °C. Anal. Calcd for $C_{59}H_{86}O_6P_2$: C, 74.33; H, 9.10. Found: C, 74.40; H, 9.09.

Preparation of 2,2′-Bis(((2,2′-bisphenoxy)phosphino)-oxy)-3,3′-di-*tert*-butyl-5,5′-dimethoxy-1,1′-biphenyl (8). 2,2′-Bisphenoxyphosphorus chloride was prepared according to a modified literature procedure.[7a] 2,2′-Bisphenol (20 g, 10.8 mmol) was dissolved in 50 mL of THF and added dropwise to a solution of PCl_3 (10 mL, 112 mmol) and NEt_3 (30 mL, 216 mmol) in 100 mL of THF at 0 °C. The mixture was allowed to cool to room temperature and subsequently refluxed for 6 h. After the mixture was cooled to room temperature, the Et_3-NHCl salts were removed by means of filtration and the solvent was removed by evaporation. The product was purified by destillation (bp 120 °C/0.2 mmHg). Yield: 13.45 g (54 mmol, 50%) of a white powder. $^{31}P[^1H]$ NMR: δ (ppm) 179.8 (s) ($CDCl_3$). ^1H NMR: δ 7.54−7.29 (m).

A solution of 4,4′-dimethoxy-6,6′-di-*tert*-butyl-2,2′-bisphenol (0.66 g, 1.84 mmol) and pyridine (1 mL, 19.09 mmol) in 25 mL of THF was added dropwise to a solution of 2,2′-bisphenoxyphosphorus chloride (0.92 g, 3.67 mmol) in 40 mL of THF at −50 °C. The solution was stirred overnight at room temperature. After filtration the solvent and the excess of pyridine were evaporated, and on addition of acetonitrile, a white precipitate was formed. The product was washed 2 times with cold acetonitrile (10 mL) and dried in vacuum. Yield: 1.14 g (1.45 mmol, 79%). $^{31}P[^1H]$ NMR: δ 146.5 ppm (s) ($CDCl_3$). ^1H NMR: δ (ppm) 1.34 (s, 18H, C_4H_9), 3.81 (s, 6H, OCH_3), 6.78−7.44 (m, 20H, arom) ($CDCl_3$). Mp: 116−119 °C. Anal. Calcd for $C_{46}H_{44}O_8P_2$: C, 70.22; H, 5.64. Found: C, 69.60; H, 5.57.

Preparation of 2,2′-Bis(((2,2′-bisphenoxy)phosphino)-oxy)-3,3′,5,5′-tetra-*tert*-butyl-1,1′-biphenyl (9). A solution of 4,4′,6,6′-tetra-*tert*-butyl-2,2′-bisphenol (0.75 g, 1.83 mmol) and pyridine (1 mL, 19.09 mmol) in 25 mL of THF was added dropwise to a solution of 2,2′-bisphenoxyphosphorus chloride (0.92 g, 3.67 mmol) at 50 °C. Subsequently, the reaction was allowed to cool down to room temperature and stirred for 2 days. The pyridine salts were removed by means of filtration, and the solvent and excess pyridine were evaporated. The product was obtained by precipitation on addition of acetonitrile, recrystallized from toluene/acetonitrile, and dried in vacuo. Yield: 1.04 g (1.24 mmol, 67.5%). $^{31}P[^1H]$ NMR: δ (ppm) 145.8 (s) ($CDCl_3$). ^1H NMR: δ (ppm) 1.37 (s, 30H, *o*-C_4H_9, *p*-C_4H_9), 6.69−7.59 (m, 20H, arom) ($CDCl_3$). Mp: 148−150 °C.

Preparation of 2,2′-bis(((4,4′,6,6′-tetra-*tert*-butyl-2,2′-bisphenoxy)phosphino)oxy)-1,1′-biphenyl (10). A solution of PCl_3 (0.6 mL, 7.40 mmol), 4,4′,6,6′-tetra-*tert*-butyl-2,2′-bisphenol (3 g, 7.32 mmol) and triethylamine (4 mL, 28.86 mmol) in 50 mL of toluene was stirred for 1 day. After filtration 2,2′-bisphenol (0.68 g, 3.66 mmol) and triethylamine (2 mL, 14.43 mmol) were added and the reaction mixture was stirred overnight. The resulting suspension was filtered, and after evaporation of the toluene and excess of NEt_3 a crude product was obtained by crystallization from toluene/acetonitrile. The product was purified by column chromatography (eluent: 5% EtOAc/toluene). Yield: 1.00 g (0.94 mmol, 26%). $^{31}P[^1H]$ NMR: δ (ppm) 137.6 (s) ($CDCl_3$). ^1H NMR: δ (ppm) 7.39 (d, 4H arom, $J = 2.43$ Hz), 7.27 (m, 2H arom), 7.20 (d, 4H arom, $J = 2.43$ Hz), 7.069 (m, 2H arom), 6.89 (m, 4H arom), 1.39 (s, 36H, *o*-C_4H_9), 1.29 (s, 36H, *p*-C_4H_9) ($CDCl_3$). Anal. Calcd for $C_{68}H_{88}O_6P_2$: C, 76.80; H, 8.35. Found: C, 76.33; H, 8.40.

Synthesis of Rhodium Diphosphite Complexes. In-Situ Preparation of Rh(CO)Acac(1). $Rh(CO)_2Acac$ (5 mg, 1.94×10^{-5} mol) and **1** (0.021 g, 1.94×10^{-5} mol) were placed in an NMR tube, and 0.3 mL of benzene-d_6 was added. The product was formed immediately as CO evolved. ^1H-NMR: δ (ppm) 1.19, 1.22, 1.25, 1.27, 1.72, 1.84 (s, 6 × 9H, C_4H_9), 1.29 (s, 2 × 9H, C_4H_9 + 3H Acac CH_3) (C_6D_6). $^{31}P[^1H]$ NMR data are listed in Table 4.

Preparation of RhAcac(1). $Rh(CO)_2Acac$ (50 mg, 1.94×10^{-4} mol) and **1** (0.21 g, 1.94×10^{-4} mol) were stirred in 4 mL of toluene for 8 h at 40 °C. The product was precipitated by addition of 5 mL of MeOH recrystallized from toluene/MeOH and dried in vacuum. Yield: 0.11 g (8.23×10^{-5} mol, 42%) of a light yellow powder. $^{31}P[^1H]$ NMR data ($CDCl_3$) are listed in Table 4. ^1H NMR: δ (ppm) 0.89, 1.12, 1.32, 1.36, 1.40, 1.42, 1.65, 1.67 (s, 8 × 9H, C_4H_9), (s, 2 × 9H, C_4H_9 + 3H Acac CH_3), 1.18 (s, 3H Acac CH_3), 5.06 (s, 1H, Acac-H), 6.37−7.53 (m, 16H, arom) ($CDCl_3$). ^{13}C NMR: δ (ppm) 26.93, 26.28 (2×, Acac CH_3), 31.69, 31.42, 32.12, 32.28, 33.47, 34.63 (18×, *t*-Bu CH_3), 31.99 (6×, *t*-Bu CH_3), 34.25, 34.94, 35.02, 35.42, 35.86, 36.25, 36.51, 37.11 (8×, *t*-Bu C), 100.11 (Acac CH), 121.23−130.50 (16×, CH arom), 128.24−151.59 (20×, C arom), 184.39, 185.97 (2×, Acac C) ($CDCl_3$). Anal. Calcd for $C_{73}H_{97}O_8P_2Rh$: C, 69.18; H, 7.72. Found: C, 69.51; H, 7.96.

Preparation of HRh(diphosphite)$(CO)_2$. In a typical experiment, $Rh(CO)_2Acac$ (10 mg, 3.878×10^{-6} mol) and diphosphite **1** (0.041 g, 3.85×10^{-6} mol) were brought into a small glass sample bottle containing a magnetic stirrer. A 2 mL volume of deuterated benzene was added. The bottle was brought into an autoclave, and after closure, the autoclave was filled with 12 bar of CO/H_2 and heated to 40 °C. After 3 h, the autoclave was cooled to room temperature and the pressure was released. The yellow/orange solution was brought into an NMR tube. Elemental analysis could not be performed because of rapid decomposition of the complex in vacuum.

In-Situ Preparation of $RhH(CO)PPh_3$(4). An NMR tube was charged with $RhH(CO)(PPh_3)_3$ (10 mg, 0.011 mmol) and 1 equiv of **4** (12.5 mg, 0.011 mmol). A 0.5 mL volume of deuterated benzene was added. The tube was heated to 40 °C and regularly shaken. After 1 h NMR was measured. Data after simulation: ^{31}P NMR δ (ppm) 160.9 (P_1), 156.3 (P_2), 34.1 (P_3 (PPh_3)), $J_{RhP1} = 250$ Hz, $J_{RhP2} = 256$ Hz, $J_{RhP3} = 140$ Hz, $J_{P1P2} = 280$ Hz, $J_{P1P3} = 177$ Hz, $J_{P2P3} = 161$ Hz; ^1H NMR δ (ppm) −10.42, $J_{HP1} = -5$ Hz, $J_{HP2} = 20$ Hz, $J_{HP3} = 9$ Hz, $J_{HRh} = 4$ Hz.

In-Situ Preparation of $RhH(CO)PPh_3$(6). The same procedure as for $RhH(CO)PPh_3$(**4**) was followed: ^{31}P NMR δ (ppm) 166.3 (P_1), 162.4 (P_2), 41.3 (P_3 (PPh_3)), $J_{RhP1} = 296$ Hz, $J_{RhP2} = 195$ Hz, $J_{RhP3} = 154$ Hz, $J_{P1P2} = 56$, $J_{P1P3} = 432$ Hz,

J_{P2P3} = 38 Hz; ^{1}H NMR δ (ppm) −5.8, J_{HP1} = 13 Hz, J_{HP2} = −191 Hz, J_{HP3} = 13 Hz, J_{HRh} = 4 Hz.

Crystallization of Rh(Acac)(4). Rh(Acac)(**4**) was prepared as Rh(Acac)(**1**) and precipitated from MeOH. Dark yellow crystals were obtained from a pentane/EtOH solution.

X-ray Structure Determination of Rh(Acac)(4). A yellow crystal with approximate dimensions 0.15 × 0.40 × 0.45 mm was used for data collection of an Enraf-Nonius CAD-4 diffractometer with graphite-monochromated Cu Kα radiation in $\omega-2\theta$ scan mode. A total of 14 136 unique reflections were measured within the range $0 \le h \le 20$, $-22 \le k \le 22$, $-16 \le l \le 15$; of these, 9433 were above the significance level of $2.5\sigma(I)$. The maximum value of $(\sin\theta)/\lambda$ was 0.59 Å^{-1}. Two reference reflections ($1\bar{1}0$, $01\bar{1}$) were measured hourly and showed 8% decrease during the 172 h collecting time, which was corrected for. Unit-cell parameters were refined by a least-squares fitting procedure using 23 reflections with $80 < 2\theta < 84°$. Corrections for Lorentz and polarization effects were applied. The structure was solved by the PATTY/ORIENT/PHASEX option of the DIRDIF94 program system.[32a] After isotropic refinement one of the *tert*-butyl groups (C(38)−C(41)) had rather high temperature factors. It was possible to distribute the three methyl groups (C(39)−C(41)) into two half-occupied positions which remained isotropic during the entire refinement. A ΔF synthesis revealed 9 peaks which were interpreted as being three molecules of ethanol, one of the solvents used during crystallization. During refinement of these solvent molecules it became apparent that their occupancy factors should be lower than 1.0; a value of 0.5 was taken for all three solvent molecules. No attempts were made to determine the hydrogen atoms of the solvent molecules. All hydrogen atom positions were calculated. Full-matrix least-squares refinement on F, anisotropic for the non-hydrogen atoms and isotropic for the hydrogen atoms restraining the latter in such a way that the distance to their carrier remained constant at approximately 1.0 Å and keeping their temperature factors fixed at U = 0.15 Å^2 (the hydrogen atoms of the disordered *tert*-butyl group were kept entirely fixed at their calculated positions), converged to R = 0.087, R_w = 0.116, $(\Delta/\sigma)_{max}$ = 0.95, and S = 1.04. A weighting scheme $w = [6.2 + 0.0129(\sigma(F_o))^2 + 0.0002/(\sigma(F_o))]^{-1}$ was used. An empirical absorption correction (DIFABS[34]) was applied, with corrections in the range 0.62−1.67. A final difference Fourier map revealed residual electron density between −1.4 and 1.3 e Å^{-3} in the vicinity of the heavy atoms. Scattering factors were taken from Cromer and Mann.[35a] The anomalous scattering of Rh, Cl, and P was taken into account.[35b] All calculations were performed with XTAL[36] unless stated otherwise. In Table 5 these data are listed. Final atomic coordinates and equivalent isotropic thermal parameters are part of the supplementary data which have been deposited at the Cambridge Crystallographic Data Centre.

Crystallization of 11. Colorless crystals were obtained by dissolving 10 mg of $Rh(CO)_2Acac$ and 44 mg of **4** in 2 mL of benzene, bringing the autoclave with its contents at 10 bar to 60 °C, releasing the pressure after 3 h, and, when most of the solvent and the obtained Hacac were evaporated, cooling the autoclave. Mp: dec >180 °C. FD MS: *m/e* 1236, [M$^+$ − 2CO − H].

X-ray Structure Determination of 11. Crystal data and details on data collection and refinement are presented in Table 7. Final atomic coordinates and equivalent isotropic thermal parameters are listed in Table 9.

A transparent, colorless crystal was mounted on a Lindemann glass capillary and transferred into the cold nitrogen stream on an Enraf-Nonius CAD4-T diffractometer on a rotating anode. Accurate unit-cell parameters and an orientation matrix were determined from the setting angles of 25 reflections (SET4).[37] Reduced-cell calculations did not indicate higher lattice symmetry.[38] Data were corrected for *Lp* effects and showed no decay for the three periodically measured reference reflections. An empirical absorption/extinction correction was applied (DIFABS[34] as implemented in PLATON[39]). The structure was solved by automated Patterson methods and subsequent difference Fourier techniques (DIRDIF-92).[33b] Refinement on F^2 was carried out by full-matrix least-squares techniques (SHELXL-93);[40] no observance criterium was applied during refinement. A disorder model is refined for one of the *tert*-butyl groups (C(18), C(19), C(20)). All non-hydrogen atoms were refined with anisotropic thermal parameters except for the disordered *tert*-butyl group. Hydrogen atoms were refined with a fixed isotropic thermal parameter amounting to 1.5 or 1.2 times the value of the equivalent isotropic thermal parameter of their carrier atoms, for the methyl hydrogen atoms and the other hydrogen atoms, respectively. On an enhanced difference map a plausible electron density was located for the hydrido atom. It was, however, not possible to refine it freely. The hydrido was placed at the initial position and not refined. It must be stressed that with this crystal structure determination it is not possible to give any certainty about either the presence or the position of the hydrido. Weights were optimized in the final refinement cycles. The structure contains a small void of 33 Å (at 0.099, 0.214, 0.544); however, no significant residual density was found in that area (PLATON/SQUEEZE).[41] Neutral atom scattering factors and anomalous dispersion corrections were taken from ref 42.

Geometrical calculations and the ORTEP illustration were performed with PLATON;[39] all calculations were performed on a DEC5000/125.

Acknowledgment. This work was supported in part (A.L.S. and N.V.) by the Netherlands Foundation of Chemical Research (SON) with financial aid from the Netherlands Organization for Scientific Research (NWO). We thank Warner van Leeuwen and Hillart Wagenmakers for their experimental assistance. We thank Jan-Meine Ernsting for the ^{103}Rh-NMR measurements.

Supporting Information Available: Tables listing X-ray parameters, fractional atomic coordinates and U values for the non-hydrogen and hydrogen atoms, anisotropic thermal parameters, and bond distances and angles for **4** and **11** (31 pages). This material is contained in many libraries on microfiche, immediately follows this article in the microfilm version of the journal, can be ordered from the ACS, and can be downloaded from the Internet; see any current masthead page for ordering information and Internet access instructions.

OM950549K

(34) Walker, N.; Stuart, D. *Acta Crystallogr.* **1983**, *A39*, 158.
(35) (a) Cromer, D. T.; Mann, J. B. *Acta Crystallogr.* **1968**, *A24*, 321. (b) Cromer, D. T.; Liberman, D. J. *J. Chem. Phys.* **1970**, *53*, 1891.
(36) Hall, S. R.; Flack, H. D.; Stewart, J. M., Eds. XTAL3.2 Reference Manual. Universities of Western Australia, Geneva and Maryland, 1992.
(37) Boer, J. L. D.; Duisenberg, A. J. M. *Acta Crystallogr.* **1984**, *A40*, C410.
(38) Spek, A. L. *J. Appl. Crystallogr.* **1988**, *21*, 578.
(39) Spek, A. L. *Acta Crystallogr.* **1990**, *A46*, C34.
(40) Sheldrick, G. M. SHELXL-93 Program for crystal structure refinement. University of Göttingen, Germany, 1993.
(41) Spek, A. L. *ACA Abstracts* **1994**, *22*, 66.
(42) Wilson, A. J. C., Ed. *International Tables for Crystallography*; Kluwer Academic Publishers: Dordrecht, The Netherlands, 1992; Vol. C.